Title
Monocarboxylate Transporter 1 modulates cancer cell pyruvate export and tumor growth

Author
Hong, Candice Sun

Publication Date
2016

Peer reviewed|Thesis/dissertation

UNIVERSITY OF CALIFORNIA

Los Angeles

Monocarboxylate Transporter 1 modulates cancer cell pyruvate export and tumor growth

A dissertation submitted in partial satisfaction of the

requirements for the degree of Doctor of Philosophy

in Molecular and Medical Pharmacology

by

Candice Sun Hong

2016

ABSTRACT OF THE DISSERTATION

Monocarboxylate Transporter 1 modulates cancer cell pyruvate export and tumor growth

by

Candice Sun Hong

Doctor of Philosophy in Molecular and Medical Pharmacology

University of California, Los Angeles, 2016

Professor Heather R. Christofk, Chair

Many cancers rely on glycolytic metabolism to fuel rapid proliferation. This has spurred interest in designing drugs that target tumor glycolysis such as AZD3965, a small molecule inhibitor of Monocarboxylate Transporter 1 (MCT1) currently undergoing Phase I evaluation for cancer treatment. Since MCT1 mediates proton-linked transport of monocarboxylates such as lactate and pyruvate across the plasma membrane (Halestrap and Meredith, 2004), AZD3965 is thought to block tumor growth through disruption of lactate transport and glycolysis. Here we show that MCT1 inhibition impairs proliferation of glycolytic breast cancer cells that express MCT4 via disruption of pyruvate rather than lactate export. We found that MCT1 expression is elevated in glycolytic breast tumors and cell lines as well as in malignant breast and lung tissues. High MCT1 expression predicts poor prognosis in breast and lung cancer patients. Stable knockdown and AZD3965-mediated inhibition of MCT1 promote oxidative metabolism. Acute inhibition of MCT1 reduces pyruvate export rate but does not consistently alter lactate transport or glycolytic flux in breast cancer cells that also express MCT4. Despite the lack of glycolysis impairment, MCT1 loss-of-function decreases breast cancer cell proliferation and blocks growth of mammary

fat pad xenograft tumors. Our data suggest that MCT1 expression is elevated in glycolytic cancers to promote pyruvate export, which when inhibited enhances oxidative metabolism and reduces proliferation. This study presents an alternative molecular consequence of MCT1 inhibitors that further supports their use as anti-cancer therapeutics.

The dissertation of Candice Sun Hong is approved

Steven J. Bensinger
Thomas G. Graeber
William Edward Lowry
Heather R. Christofk, Committee Chair

University of California, Los Angeles,
2016

For my family,
JH

Table of contents

List of Figures and Tables

Acknowledgements

Many exceptional people contributed to this work and to my graduate student experience. I'd first like to thank all the members of the Christofk lab, past and present who contributed to the project. First, I'd like to thank Wen Gu for being an amazing bay-mate and friend these past 6 years. Thank you for letting me borrow your pipettes and things off your bench without complaint. I'd like to thank Carolina Espindola who was my extra set of hands while I couldn't be in lab. Thank you for always being willing to help and always doing it with a smile.

Next I'd like to thank my dad, Dr. Eung-Kwon Pae, who first started me down this science path. Thank you for your advice and proof reading all my work. Thank you so much for surprising me and coming to my defense all the way from Baltimore.

I'm so grateful for my mom, Joy Pae, who helped raise my children while I finished my graduate work. Thank you for raising us, thank you for raising my kids.

I'd also like to thank my husband, Johnny Hong, for always believing in me and my work. Thank you for waking up every morning with the kids (Judah and Josiah) so I can get extra sleep. I love you!

Lastly, I'd like to thank my mentor Dr. Heather Christofk. You have been an amazing mentor to me both inside and out of lab. I would not have gone to graduate school if it hadn't been my interested in your research. I would not have stayed in graduate school if it hadn't been for your kindness and support after Judah was born. I would not be writing this today if it hadn't been for all your guidance and advice on my project. It has been an honor and privilege to have been part of your lab.

The work for this dissertation was performed under the direction of Dr. Heather R. Christofk

Chapter 1

This chapter is based upon work from the manuscript Hong, C.S., Graeber, T.G., Christofk, H.R. Monocarboxylate Transporter 1 modulates cancer cell pyruvate export and tumor growth. Submitted, *Cell Reports*

Chapter 2

This chapter is based upon work from the manuscript Hong, C.S., Graeber, T.G., Christofk, H.R. Monocarboxylate Transporter 1 modulates cancer cell pyruvate export and tumor growth. Submitted, *Cell Reports*

Chapter 3

This chapter is based upon work from the manuscript Hong, C.S., Graeber, T.G., Christofk, H.R. Monocarboxylate Transporter 1 modulates cancer cell pyruvate export and tumor growth. Submitted, *Cell Reports*

Vita

Education

2006 B.S. Molecular, Cell and Developmental Biology
Minor East Asian Languages and Cultures
University of California, Los Angeles

Publications and Presentations

Hong, C.S., et al.(2015) Monocarboxylate Transporter 1 modulates cancer cell metabolic metabolism and proliferation. *Preparing for submission to Cancer Metabolism.*

Garon, E. B., Christofk, H. R., Hosmer, W., Britten, C. D., Bahng, A., Crabtree, M. J., **Hong, C. S**., et al. (2014). Dichloroacetate should be considered with platinum-based chemotherapy in hypoxic tumors rather than as a single agent in advanced non-small cell lung cancer. *Journal of cancer research and clinical oncology*. doi:10.1007/s00432-014-1583-9

McBrian, M. a, Behbahan, I. S., Ferrari, R., Su, T., Huang, T.-W., Li, K., **Hong, C. S**., et al. (2013). Histone acetylation regulates intracellular pH. *Molecular cell*, *49*(2), 310–21. doi:10.1016/j.molcel.2012.10.025

Cummings, D. M., Alaghband, Y., Hickey, M. a, Joshi, P. R., **Hong, S. C.**, Zhu, C., Ando, T. K., et al. (2012). A critical window of CAG repeat-length correlates with phenotype severity in the R6/2 mouse model of Huntington's disease. *Journal of neurophysiology*, *107*(2), 677–91. doi:10.1152/jn.00762.2011\

Introduction

Glucose metabolism and Cancer

Cellular metabolism

Despite what many people think these days, the main purpose of eating food isn't for enjoyment, but for energy. As we consume food, our digestive system breaks down these nutrients into smaller and smaller molecules, which then get absorbed into our cells to be converted into energy, otherwise known as adenosine triphosphate (ATP). From the beating of our hearts, to the firing of neurons, our bodies require energy to function. On a cellular basis this can mean transporting molecules, growing and dividing, and general housekeeping functions.

Eukaryotic cells have the ability to harvest energy via different metabolic pathways such as glycolysis, or the citric acid cycle and oxidative phosphorylation (OXPHOS). In the 1860s Louis Pasteur observed that in the absence of oxygen, energy is produced by glycolysis (2 molecules ATP/molecule of glucose), whereas in the presence of oxygen, glucose is metabolized more efficiently by OXPHOS to produce much more energy (32 molecules ATP/molecule of glucose). Interestingly, in the 1920s Otto Warburg made the observation that cancer cells predominantly metabolize glucose by glycolysis even in the presence of oxygen, and this phenomenon is called the Warburg effect or aerobic glycolysis (Warburg, O, 1956). This dysregulation of cellular energetics has been observed in the majority of cancers is considered a hallmark of cancer (Hanahan and Weinberg, 2013). The fact that altered energy metabolism is also intertwined with the other hallmarks (ex.angiogenesis, metastasis), makes it a unique and effective target for cancer therapy (Kroemer and Pouyssegur, 2008). Currently it is thought that cancer cells obtain this glycolytic phenotype in order to build biomass for a proliferative advantage (Vander Heiden, 2009).

Targeting cancer metabolism

Since the 1980s, the Warburg effect has been taken advantage of in clinics to image glycolytic tumors via FDG-PET (2-deoxy-2-[^{18}F]fluoro-D-glucose positron emission tomography) for cancer diagnosis (Czernin, J., & Phelps, M. E. (2002). In the recent decade, further work in cancer metabolism has identified several possible targets in different metabolic circuitries for therapeutics. Furthermore, drugs designed for other metabolic diseases have now returned to clinical trials to test their effects on cancer (Galluzi, 2013). For example, metformin and phenformin are biguanides that target mitochondrial complex I currently used to treat type II diabetes. Retrospective epidemiology studies found evidence that diabetic patients on metformin had a decreased risk of cancer incidence (Evans et al., 2005). Metformin is currently undergoing several phase II and phase III clinical chemoprevention studies.

Despite much preclinical data suggesting possible metabolic targets, few are currently in clinical development. A small molecule inhibitor targeting choline kinase is currently in clinical development to treat patients with solid tumors, and completed its first phase I clinical trial in 2014 (Galluzi, 2013). Choline kinase is often upregulated in cancer as its product phosphocholine is necessary to produce phosphotidylcholine which is essential to create membranes (Clem, 2011). The inhibitor (TCD-717) is novel in that it targeted phospholipid metabolism, and therefore rapidly proliferating cells. Another drug currently in phase I clinical trials is an inhibitor that targets a monocarboxylate transporter I (MCT1) that has been found to be upregulated in many cancers (Polanski et al., 2014). Further clinical studies of other targets, alone or in conjunction with current therapies, will be needed to determine the efficacy of these more selective cancer therapy agents that target the unique metabolic signatures of cancer cells .

Monocarboxylate Transporter I

Monocarboxylates are produced and utilized in key roles in metabolism and must be transported across the plasma membrane and the inner mitochondrial membrane (Halestrap 2012). A family of monocarboxylate transporters (MCTs) takes on these roles in different tissues of the body. The MCT family has 14 different isoforms, but MCT1-4 in particular are known to catalyze the bidirectional transport of monocarboxylates across the plasma membrane coupled with a proton (Figure 1) (Halestrap 2012). All 14 membranes have conserved sequences and it has been found that the transporters have 12 transmembrane domains with intracellular C and N termini (Figure 2). Some MCTs, like MCT1 and MCT4 require the presence of an ancillary protein called CD147 to be correctly expressed on the plasma membrane (Halestrap 2012). MCTs can be regulated at transcriptional or post-transcriptional levels (Halestrap and Wilson, 2012).

MCT1 inhibitors were first designed when it was found that blocking MCT1 induction during T cell activation blocked T cell division (Murray et al., 2005), and therefore could act as an immunosuppressant drug. In recent years there has been much interest in using MCT1 as a target for cancer therapy as MCT1 has been found to be upregulated in many cancers (Pinheiro et al., 2008, Pinheiro et al., 2010, Curry et al.. 2013, Izumi et al., 2011). Currently an MCT1 inhibitor (AZD3965) is undergoing phase I evaluation in the United Kingdom for patients with solid tumors, prostate cancer, gastric cancer, and diffuse large cell B lymphoma (Polanski et al., 2014).

Conclusion

Our interest in MCT1 stemmed from our preliminary data that found that MCT1 was the most strongly correlated gene with glycolytic phenotype breast cancer patient tumors, and glycolytic breast cancer cell lines. We proposed to test the hypothesis that altering the metabolic state of cancer cells can affect tumor development and progression. We hypothesized that one such metabolic regulator was MCT1, and that it is important for the Warburg effect and breast cancer cell proliferation.

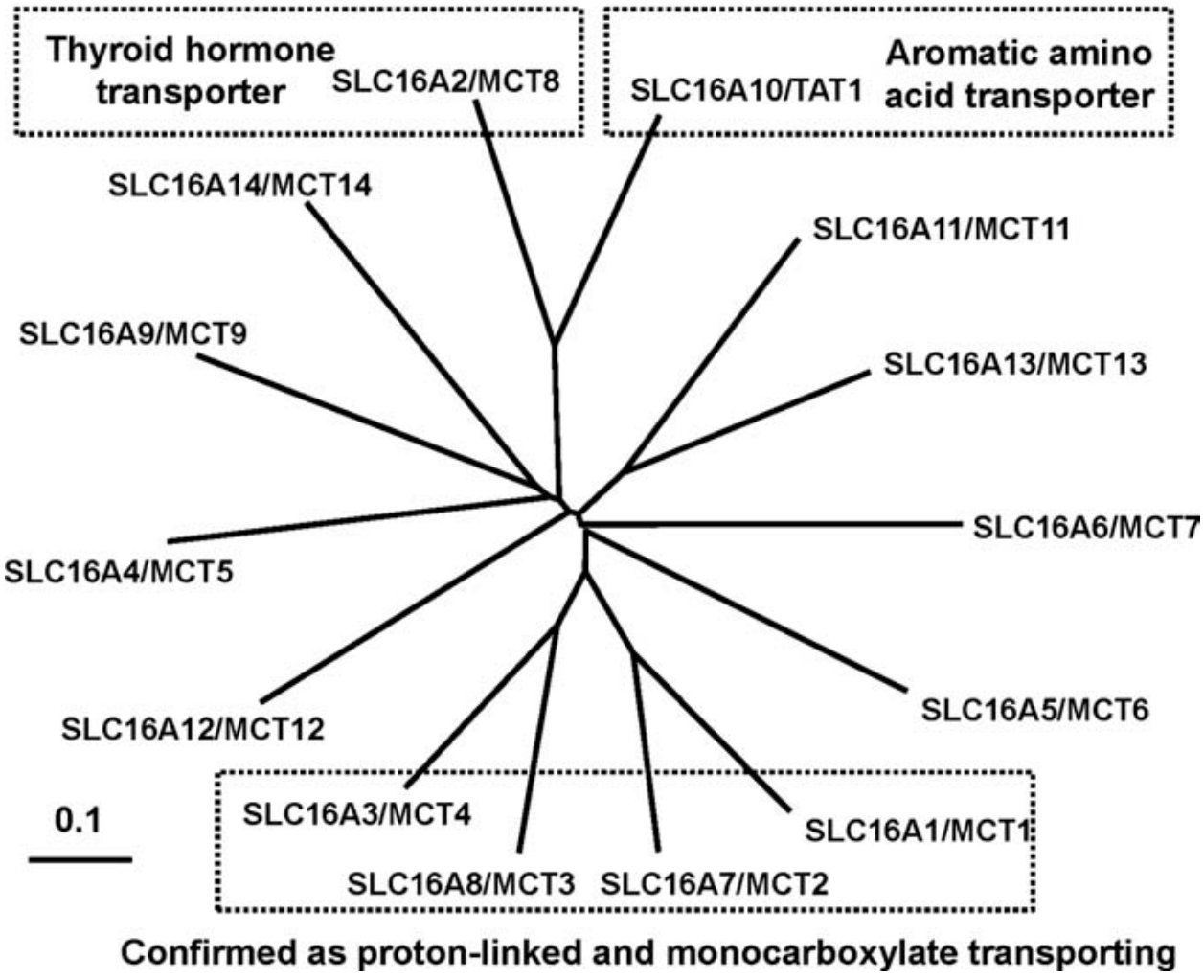

Figure 1. Phylogenetic tree of MCT family.

A.

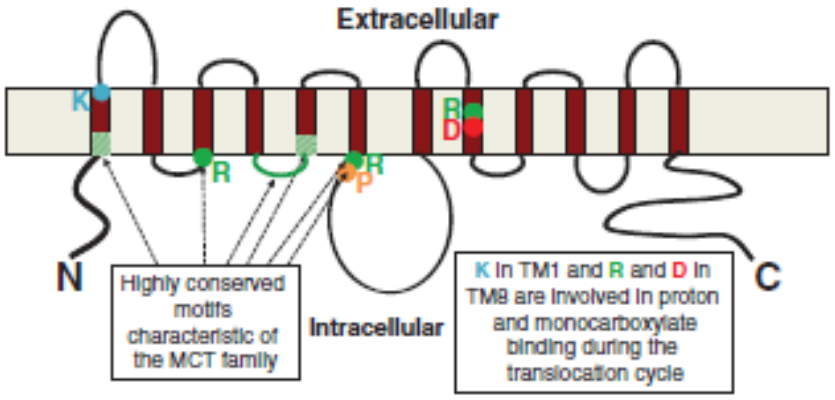

B.

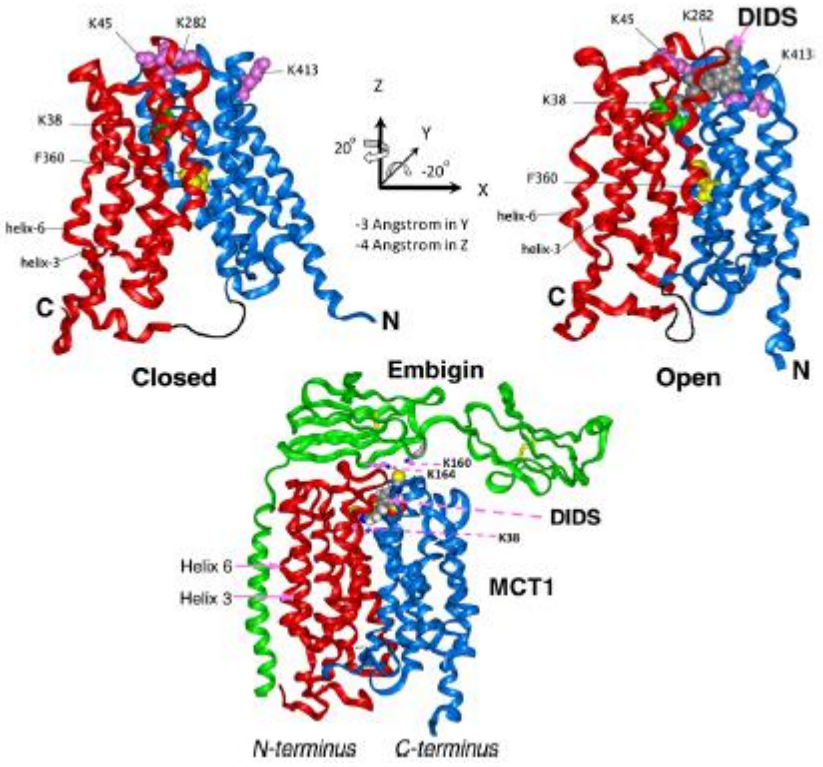

Figure 2. Predicted structures of MCTs. a., Conserved characteristics of MCTs include 12 TM domains and intracellular N and C termini. **b.,** Proposed crystal structure of MCT1.

References

Clem, B. F., Clem, a L., Yalcin, a, Goswami, U., Arumugam, S., Telang, S., Trent, J. O., et al. (2011). A novel small molecule antagonist of choline kinase-α that simultaneously suppresses MAPK and PI3K/AKT signaling. *Oncogene*, *30*(30), 3370–80. doi:10.1038/onc.2011.51

Curry, J. M., Whitaker-menezes, D., Ames, J. A., Anantharaman, A., Butera, A., Leiby, B., Cognetti, D. M., et al. (2013). MCT1 and MCT4 are functional biomarkers of metabolic symbiosis in head and neck cancer Cancer metabolism , stemness and tumor recurrence, 1371–1384.

Czernin, J., & Phelps, M. E. (2002). P OSITRON E MISSION T OMOGRAPHY S CANNING : Current and Future Applications, 89–112.

Evans Josie M M, Donnelly Louise A, Emslie-Smith Alistair M, Alessi Dario R, Morris Andew D. Metformin and reduced risk of cancer in diabetic patients. BMJ 2005; :bmj;bmj. 38415.708634.F7v1

Galluzzi, L., Kepp, O., Vander Heiden, M. G., & Kroemer, G. (2013). Metabolic targets for cancer therapy. *Nature reviews. Drug discovery*, *12*(11), 829–46. doi:10.1038/nrd4145

Halestrap, A. P. (2012). The monocarboxylate transporter family--Structure and functional characterization. *IUBMB life*, *64*(1), 1–9. doi:10.1002/iub.573

Halestrap, A.P., and Wilson, M.C. (2012). The monocarboxylate transporter family--role and regulation. IUBMB Life *64*, 109-119.

Hanahan, D., & Weinberg, R. a. (2011). Hallmarks of cancer: the next generation. *Cell*, *144*(5), 646–74. doi:10.1016/j.cell.2011.02.013

Izumi, H., Takahashi, M., Uramoto, H., Nakayama, Y., Oyama, T., Wang, K.-Y., Sasaguri, Y., et al. (2011). Monocarboxylate transporters 1 and 4 are involved in the invasion activity of human lung cancer cells. Cancer science, 102(5), 1007–13. doi:10.1111/j.1349-7006.2011.01908.x

Kroemer, G., & Pouyssegur, J. (2008). Tumor cell metabolism: cancer's Achilles' heel. *Cancer cell*, *13*(6), 472–82. doi:10.1016/j.ccr.2008.05.005

Murray CM, Hutchinson R, Bantick JR, Belfield GP, Benjamin AD, Brazma D, Bundick RV, Cook ID, Craggs RI, Edwards S, Evans LR, Harrison R, Holness E, Jackson AP, Jackson CG, Kingston LP, Perry MW, Ross AR, Rugman PA, Sidhu SS, Sullivan M, Taylor-Fishwick DA, Walker PC, Whitehead YM, Wilkinson DJ, Wright A, Donald DK. Monocarboxylate transporter MCT1 is a target for immunosuppression. *Nat Chem Biol*. 2005 Dec;1(7):371-6.

Pinheiro, C., Longatto-Filho, A., Scapulatempo, C., Ferreira, L., Martins, S., Pellerin, L., Rodrigues, M., et al. (2008). Increased expression of monocarboxylate transporters 1, 2, and 4 in colorectal carcinomas. *Virchows Archiv : an international journal of pathology*, *452*(2), 139–46. doi:10.1007/s00428-007-0558-5

Pinheiro, C., Albergaria, A., Paredes, J., Sousa, B., Dufloth, R., Vieira, D., Schmitt, F., et al. (2010). Monocarboxylate transporter 1 is up-regulated in basal-like breast carcinoma. *Histopathology*, *56*(7), 860–7. doi:10.1111/j.1365-2559.2010.03560.x

Polanski, R., Hodgkinson, C.L., Fusi, A., Nonaka, D., Priest, L., Kelly, P., Trapani, F., Bishop, P.W., White, A., Critchlow, S.E., et al. (2014). Activity of the monocarboxylate transporter 1 inhibitor AZD3965 in small cell lung cancer. Clin Cancer Res *20*, 926-937

Vander Heiden, M. G., Cantley, L. C., & Thompson, C. B. (2009). Understanding the Warburg effect: the metabolic requirements of cell proliferation. *Science (New York, N.Y.)*, *324*(5930), 1029–33. doi:10.1126/science.1160809

Warburg, O. On the origin of cancer cells. *Science* **123**, 309–314 (1956)

Chapter 1

MCT1 levels correlate with glycolytic metabolism and malignancy in breast cancer

INTRODUCTION

The altered metabolism of cancer cells known as the Warburg effect has been well established since its initial discovery in the 1920s (Warburg, O, 1956). Recent interest in cancer metabolism has been due to the growing evidence that mutations in oncogenes affect metabolism (Bensinger, S. J., & Christofk, H. R. (2012), and that glycolytic genes are one of the most upregulated gene sets in cancer (Altenberg, B., & Greulich, K. O. 2004). Furthermore, patient tumors with this kind of metabolic phenotype can be imaged by FDG-PET (2-deoxy-2-[^{18}F]fluoro-D-glucose positron emission tomography) for diagnosis, staging, and therapy response (Czernin, J., & Phelps, M. E. (2002). These advancements in the field suggest that not only can these altered metabolic pathways be ideal targets for therapy, but also that FDG-PET can be used to facilitate drug development (Kelloff, G. J., 2005). Currently the repertoire of "metabolic regulator" genes that contribute to this glycolytic metabolism are still to be determined (Bensinger, S. J., & Christofk, H. R. (2012).

In this study, we investigated the gene expression pattern of glycolytic breast cancer tumors and glycolytic breast cancer cell lines to identify potential "metabolic regulators". In finding the transcript for the solute carrier 16A1 (SLC16A1) encoding the protein monocarboxylate transporter 1 (MCT1) highly correlated with glycolytic tumors and breast cancer cells, we further analyzed the other monocarboxylate transporters (MCT1-4) mRNA expression patterns. Next we assessed MCT1 protein levels in different stage breast and lung cancer tumors, and its role in patient prognosis. Finally, we measured serum pyruvate and lactate levels from stage I and stage IV lung and breast cancer patients to determine to further validate MCT1's role *in vivo* in tumor development.

RESULTS

Glycolytic tumors and cell lines exhibit a gene expression pattern consistent with the Warburg effect

In order to identify specific transcriptional events that correlate with glycolytic phenotype in breast cancer, we analyzed gene expression profiles from eleven patient breast tumors stratified by FDG uptake and thirty-one breast cancer cell lines that we stratified based on glycolytic versus oxidative phenotype (nmol lactate produced / nmol oxygen consumed) (Fig. 1-1) (Neve et al., 2006; Palaskas et al., 2011). As shown in Figure 1-2, tumors with high FDG uptake exhibit a distinct transcriptional signature from those with low FDG uptake. Gene Set Enrichment Analysis confirmed that MYC-regulated gene sets are significantly enriched in the glycolytic breast tumors and cell lines (Figure 1-3, Table 1) (Palaskas et al., 2011). Additionally, Kyoto Encyclopedia of Genes and Genomes (KEGG) pathways involved in nucleotide metabolism and glycolysis are also enriched in the glycolytic tumors and cell lines (Fig. 1-2, Table 2) (Kanehisa et al., 2014). Consistent with previous findings (Palaskas et al., 2011), the glycolytic tumor and cell line gene expression signature significantly correlates with the basal gene expression signature in breast cancer (Chang et al., 2005) (Figure 1-4). Mapping the glycolytic gene expression signature to the KEGG glycolysis pathway demonstrates coordinated upregulation of glycolytic genes including HK2, PFKP, BPGM, ENO3 and LDHB (Figure 1-5). Together, these data demonstrate that glycolytic tumors and cell lines exhibit a gene expression signature consistent with the Warburg effect.

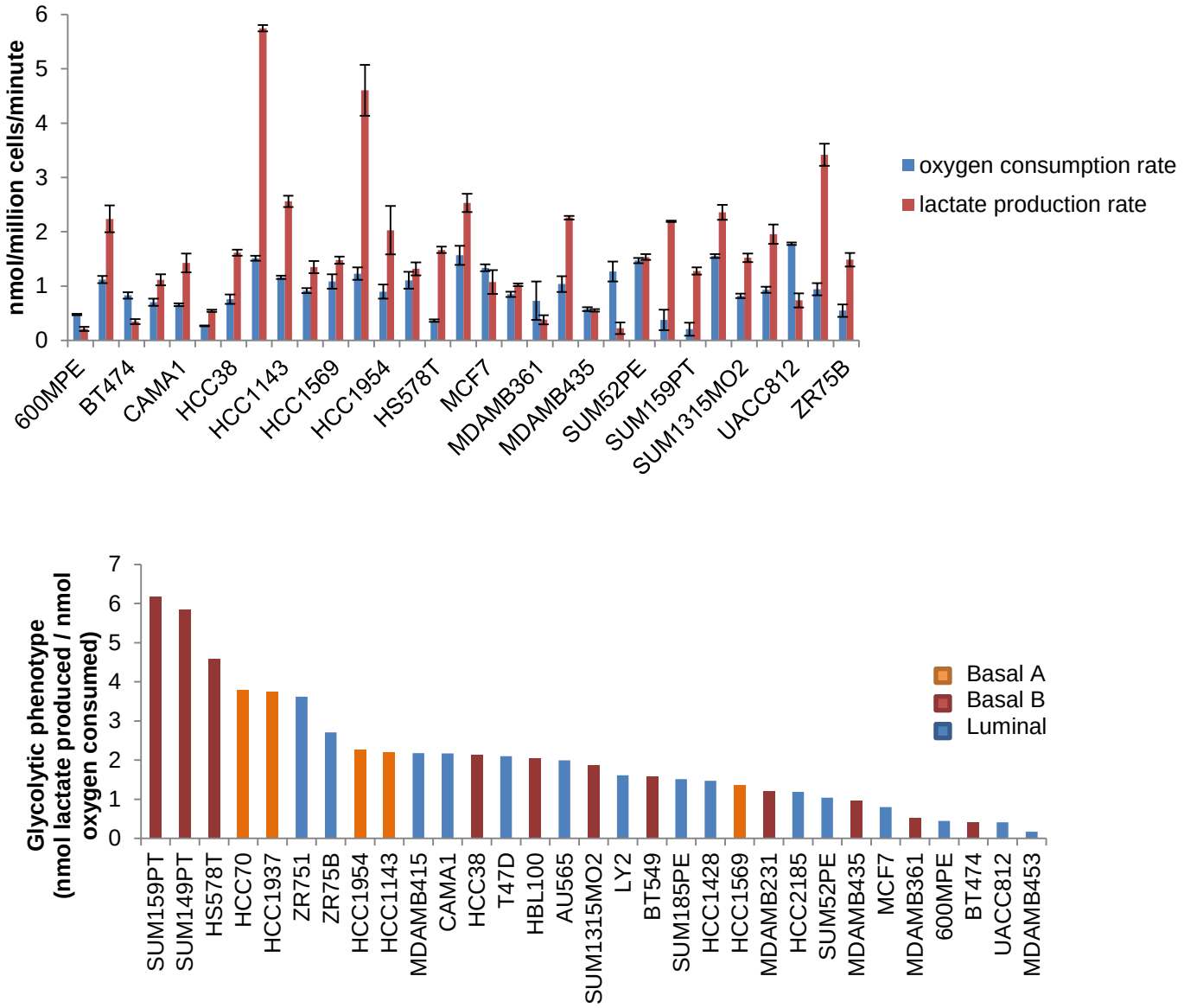

Figure 1-1. **Lactate production and oxygen consumption rates vary across a panel of 31 breast cancer cell lines.** **a**, Oxygen consumption rates (blue) and lactate production rates (red) of 31 breast cancer cell lines. Error bars denote standard deviation (n = 3). **b,** Stratification of the breast cancer cell lines based on glycolytic phenotype (nmol lactate produced / nmol oxygen consumed). Cell lines with gene expression profiles that cluster with Basal A breast cancers are indicated by orange bars, those that cluster with Basal B breast cancers are indicated by red bars, and those that cluster with Luminal breast cancers are indicated by blue bars.

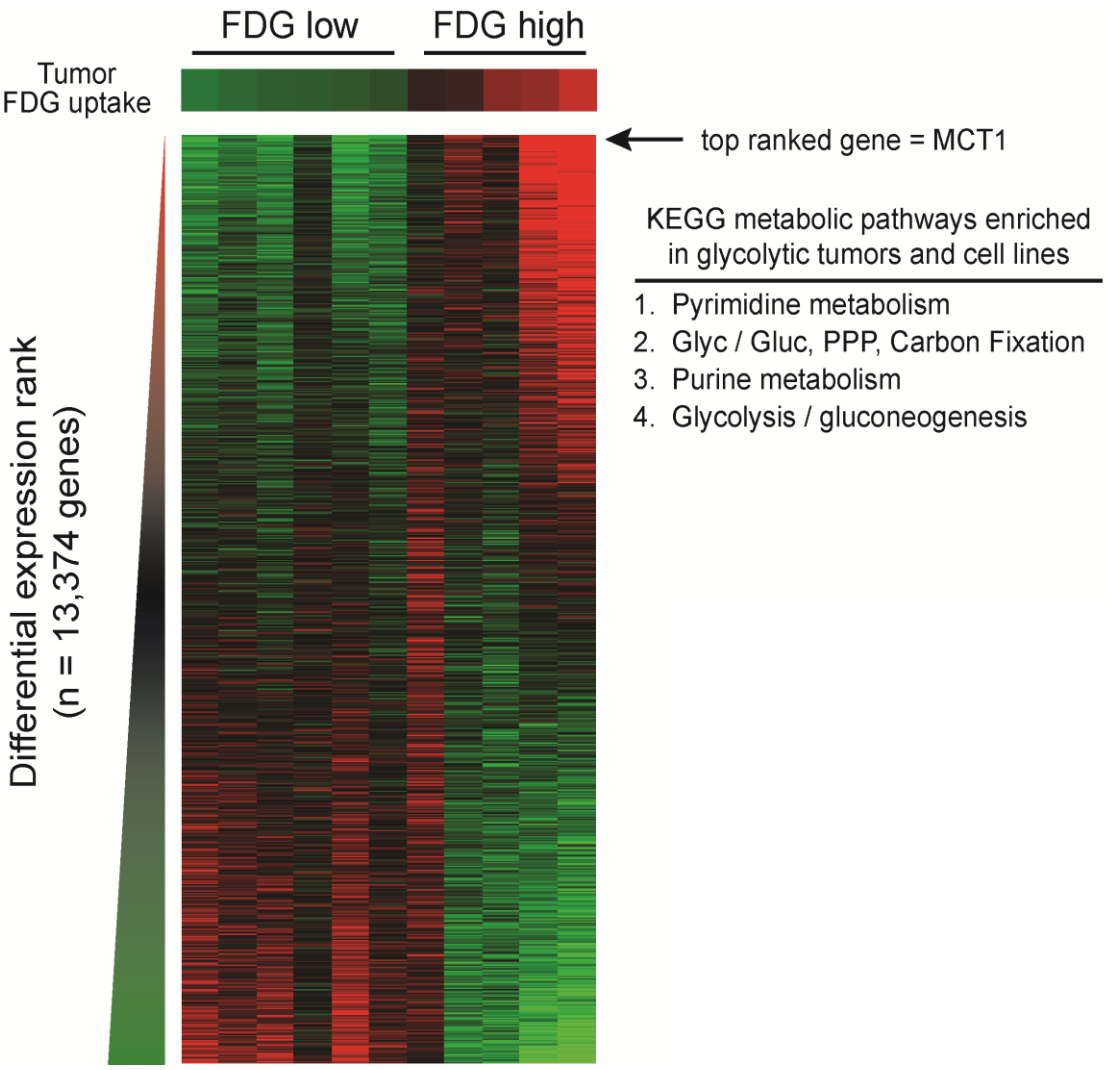

Figure 1-2. Breast tumors with high and low FDG uptake have distinct gene expression signatures. Transcript levels from 11 human breast cancers were ranked by the average correlation with tumor FDG maximum standardized uptake value (SUVmax) and cell line glycolytic phenotype (nmol lactate produced / nmol oxygen consumed) and arranged from left to right in order of increasing FDG uptake. Red and green denote high and low average correlation coefficients, respectively. MCT1 is the top-ranked of 13,374 genes. The inset table lists metabolic pathways enriched in highly glycolytic tumors and cell lines (PPP, pentose phosphate pathway; Glyc / Gluc, glycolysis / gluconeogenesis).

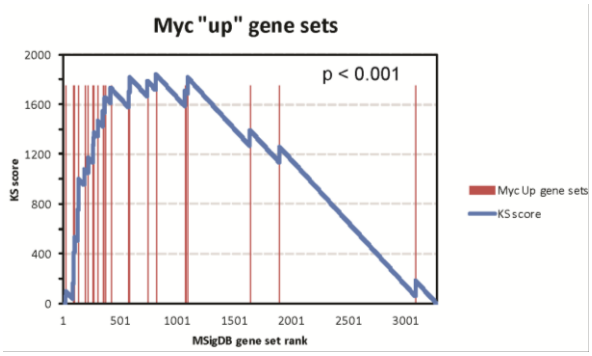

Figure 1-3 MYC-regulated gene sets are significantly enriched in the highly glycolytic breast tumors and cell lines. RNA expression data sets from i) human breast cancers with measured FDG uptake and ii) human breast cancer cell lines with measured glycolytic phenotype were analyzed individually by GSEA. Pathways from the Molecular Signatures Database (MSigDB) C2 collection were ranked by the average normalized enrichment score (NES) across the two data sets. Within this ranked list, gene sets associated with upregulated Myc activity (Myc "up") were significantly enriched in the highly glycolytic breast tumors and cell lines ($p < 0.001$). Myc "down" gene sets were not significantly enriched in either direction.

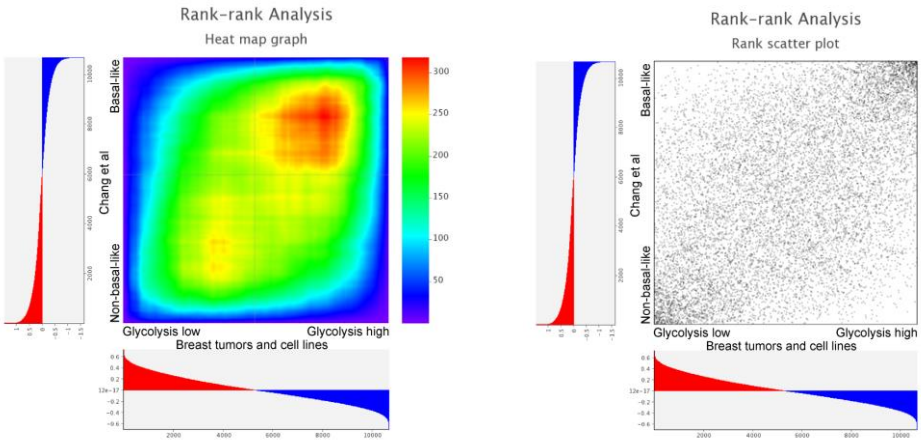

Figure 1-4. The glycolytic tumor and cell line gene expression signature correlates with basal gene expression signature in breast cancer. a, b, A ranked list of transcripts correlating with glycolytic phenotype in breast tumors and cell lines was compared to a ranked list of transcripts correlating with basal phenotype in breast cancer using the rank-rank hypergeometric overlap (RRHO) algorithm. The resulting overlap from the ranked lists, represented as a hypergeometric heat map (**a**) and a scatter plot (**b**), indicates significant correlation between the gene signatures for glycolytic and basal phenotypes in breast cancer (p-value = 10^{-300}; -log p-value = 300).

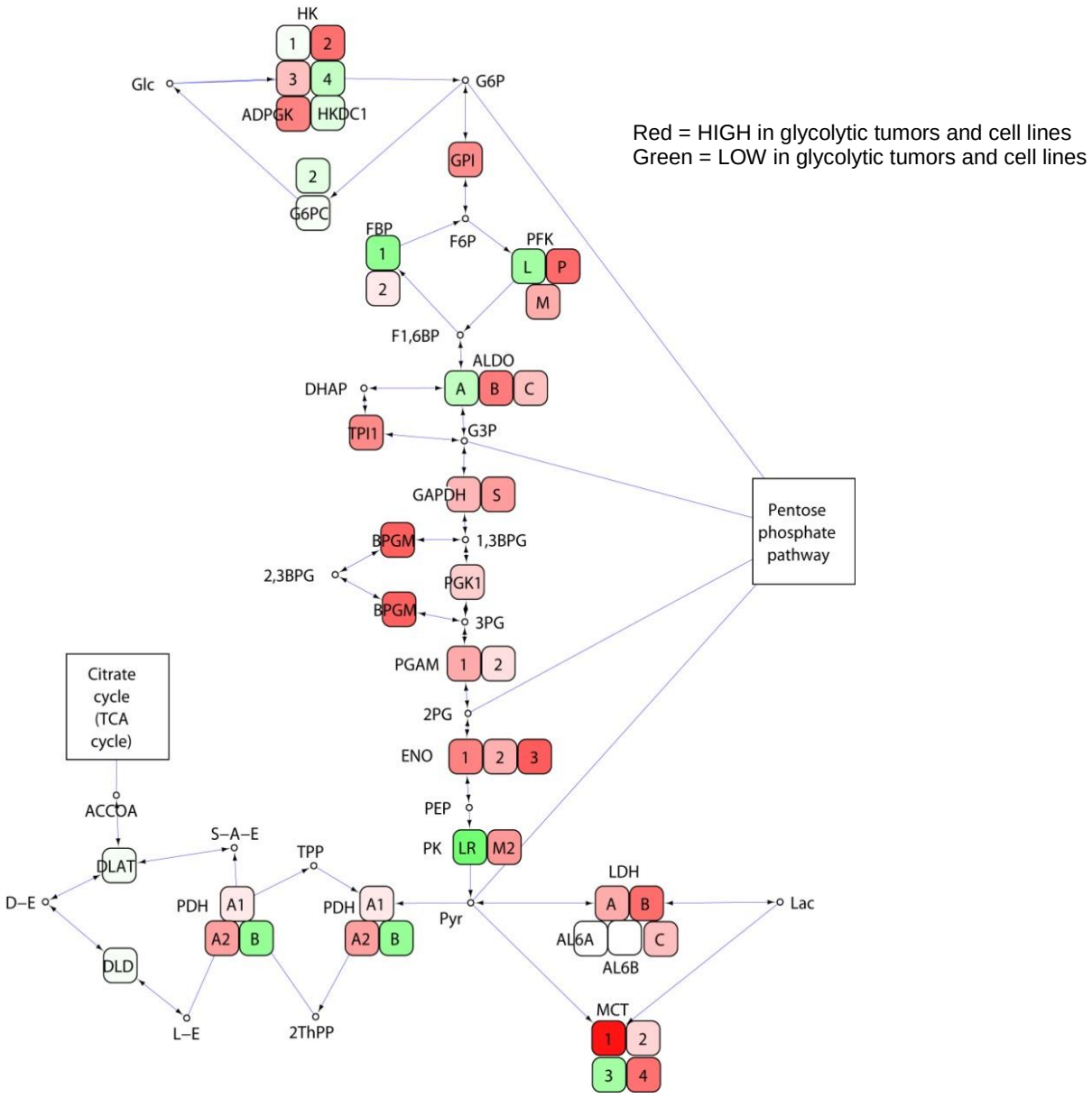

Figure 1-5. Highly glycolytic tumors and cell lines demonstrate coordinate upregulation of glycolysis genes and MCT1. Genes within the glycolysis pathway are colored red or green to denote high and low correlation coefficients with glycolytic phenotype, respectively.

MCT1 mRNA expression is strongly correlated with the glycolytic phenotype

Notably, the top ranked transcript correlating with glycolytic phenotype in breast tumors and cell lines is Solute Carrier 16A1 (SLC16A1), encoding MCT1 (Figure 1-1, Figure 1-5). Since MCT1-4 mediate monocarboxylate transport in cells, we analyzed mRNA expression patterns of the corresponding genes in breast tumors and cell lines (Figure 1-6). Only MCT1 mRNA expression yields consistently strong correlation coefficients with glycolytic phenotype in both breast tumors and cell lines (Figure 1-6). In contrast, MCT4 mRNA expression is less correlated with glycolytic phenotype (Figure 1-6). However, MCT1-4 mRNA levels in cancer cells may not reflect protein levels or transporter activity, especially since MCT4 mRNA levels have been shown to correlate poorly with protein levels in muscle (Bonen et al., 2000).

MCT1 protein levels are elevated in malignant breast and lung cancer lesions

To determine whether MCT1 protein expression is elevated in primary cancers, we analyzed normal and malignant breast and lung tissues by immunohistochemistry using high-density tissue microarrays (TMAs). MCT1 protein expression is significantly increased in malignant breast and lung tissues compared to adjacent non-malignant tissues (Figure 1-7). Later stage lung cancers (Stage II-IV) have greater MCT1 expression than those in early stages (Stage I) (integrated intensity = 0.44 ± 0.08 in Stage II-IV ($n = 174$) versus integrated intensity = 0.29 ± 0.03 in Stage I ($n=216$), $p < 0.01$). Additionally, high MCT1 expression is associated with worse prognosis in breast and lung cancer patients (Figure 1-8). These findings corroborate published results showing MCT1 elevation in basal-like breast carcinoma (Pinheiro et al., 2010) and colorectal carcinomas (Pinheiro et al., 2008) as well as studies showing association of MCT1 expression with poor prognosis in epithelial ovarian cancer (Chen et al., 2010) and gastric cancer

(Pinheiro et al., 2009). These results are inconsistent with a previous report that did not find elevated MCT1 expression by immunohistochemistry in lung adenocarcinomas (McCleland et al., 2013). One potential explanation for this discrepancy is the use of more lung adenocarcinoma patient samples in our study (715 versus 226). Additionally, while we found significantly elevated MCT1 expression in lung adenocarcinomas compared to adjacent non-malignant tissue, we found an even greater increase in MCT1 expression in squamous cell and large cell carcinoma tissues.

Serum lactate and pyruvate levels are elevated in late stage lung cancer patients

Furthermore, we found that serum lactate and pyruvate concentrations are significantly elevated in Stage IV versus Stage I lung cancer patients (Figure 1-9), consistent with MCT1 modulation of tumor cell lactate and pyruvate export *in vivo*. However, no significant difference in lactate or pyruvate levels was observed in serum from Stage IV versus Stage I breast cancer patients (data not shown).

A.

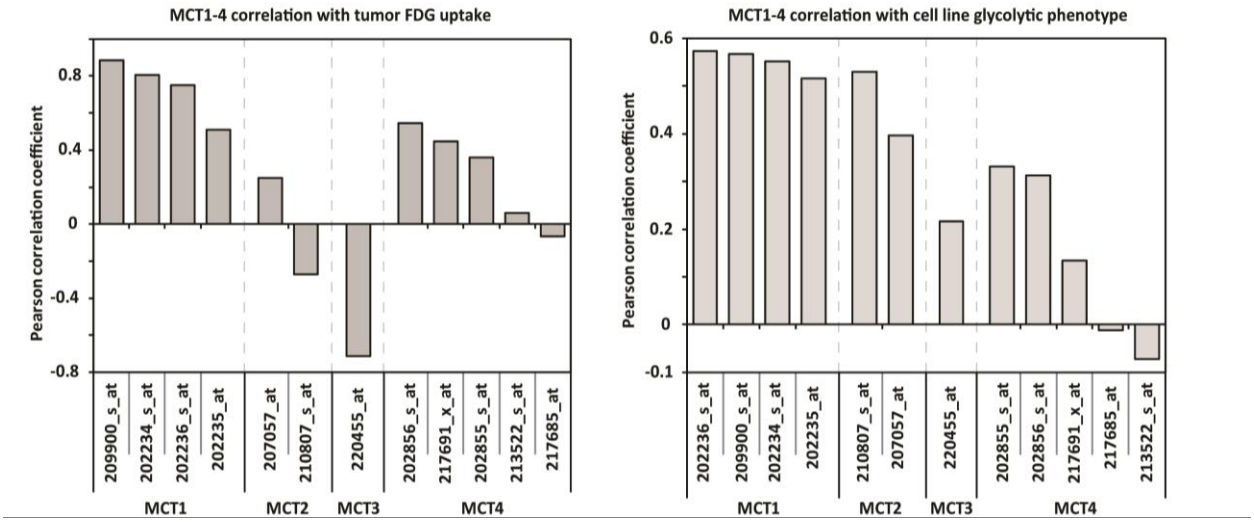

B.

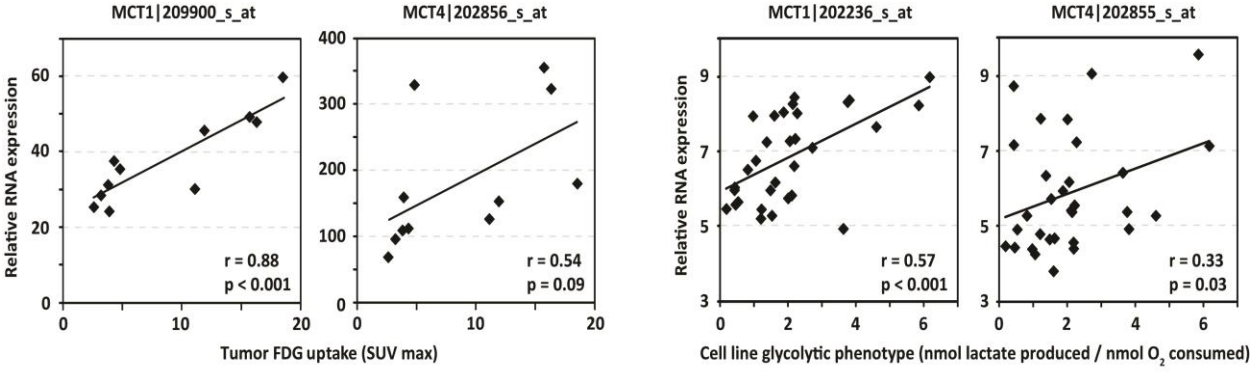

Figure 1-6. Levels of MCT1, but not other MCT family members, are highly correlated with glycolytic phenotype in breast tumors and cell lines. The Pearson correlation coefficient with FDG uptake in human breast tumors (left) and glycolytic phenotype in human breast cancer cell lines (right) is depicted for microarray probes recognizing MCT1-4 family members. **d,** Scatter plots of MCT1 and MCT4 expression demonstrate that MCT1 but not MCT4 is highly correlated with glycolytic phenotypes. Transcript levels are plotted versus FDG uptake for human breast tumors (left) and glycolytic phenotype for human breast cancer cell lines (right). P-values are the two-tailed significance of the Pearson correlation coefficient.

A.

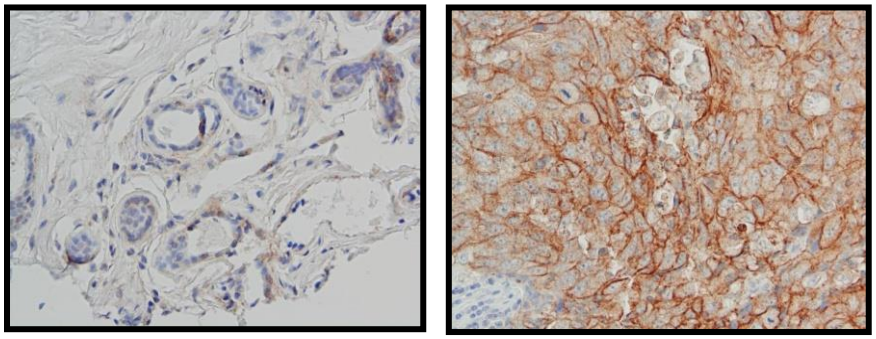

B.

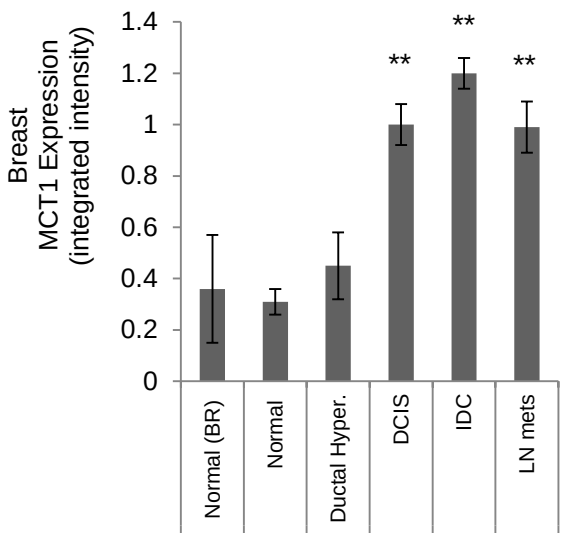

C.

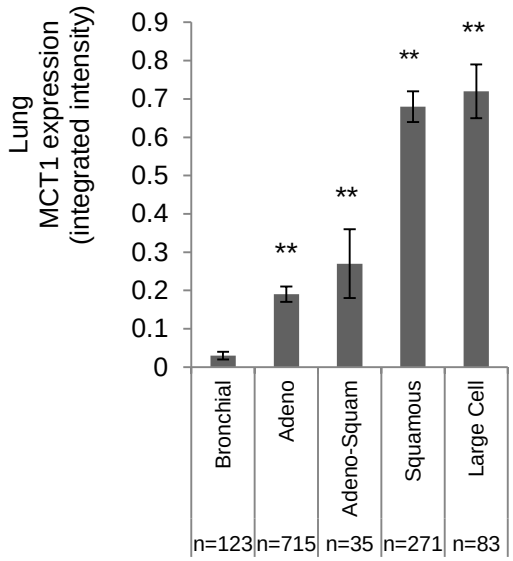

Figure 1-7. Elevated MCT1 protein levels are indicative of tumor. a, IHC of human normal breast and breast invasive ductal carcinoma (IDC) with an antibody towards MCT1. Images are shown at X 100 magnification. **b,** The mean integrated MCT1 expression as determined by immunohistochemistry on a breast tissue microarray is compared across breast histologies and histopathologies. **c,** The mean integrated MCT1 expression as determined by immunohistochemistry on a lung tissue microarrary is compared across lung histologies and histopathologies. For **b, c,** error bars denote standard error of the mean, and n = number of tissue array spots analyzed.

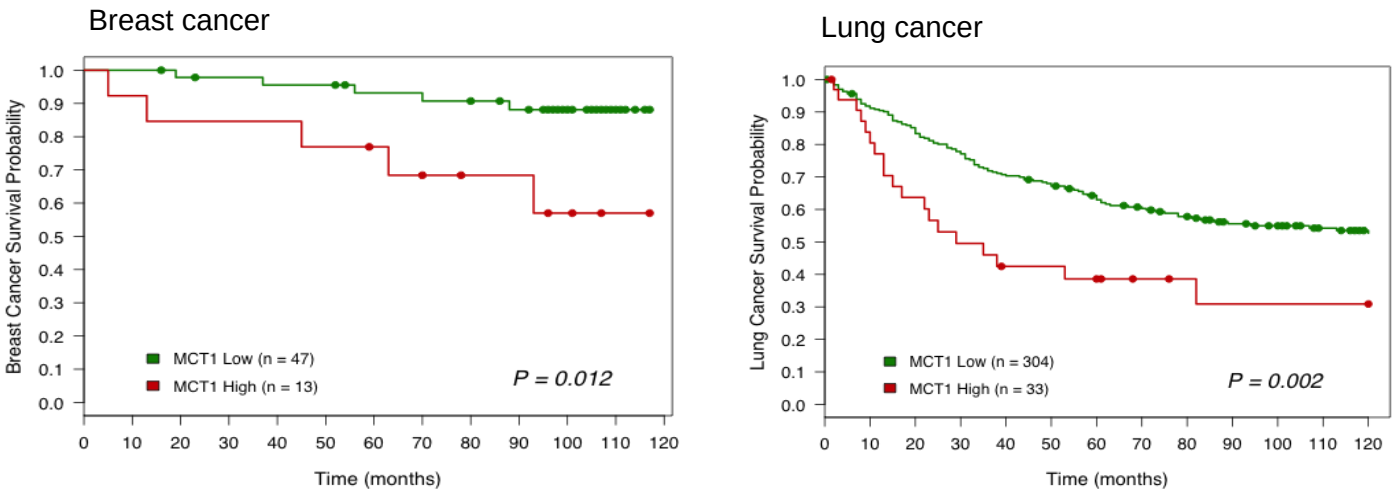

Figure 1-8. Higher MCT1 expression levels predicts poorer survival in patients. Kaplan-Meier survival plot shows patients with lower MCT1 expression (< 2.0 mean integrated intensity) depicted as a green line, and higher MCT1 expression (≥ 2.0 mean integrated intensity) depicted as a red line.

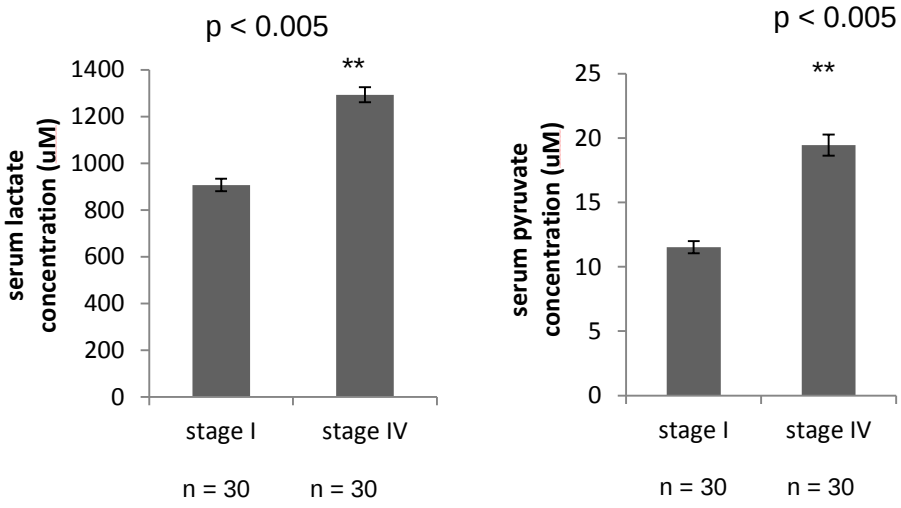

Figure 1-9. Increased serum lactate and pyruvate concentrations from lung cancer patients. Serum lactate (left) and pyruvate (right) concentrations from Stage I versus Stage IV lung cancer patients. N = number of individuals in each category.

DISCUSSION

In the present study, we investigated transcriptional changes that occur to support the Warburg effect in breast tumor and breast cancer cell lines.

We showed that tumors with high FDG uptake exhibit a distinct transcriptional signature compared to tumors with low FDG uptake. Consistent with previous reports we found that glycolysis and glycolysis related pathways to show the greatest transcriptional enrichment (Palaskas et al., 2011). Furthermore, we found that in both glycolytic breast tumors and breast cancer cell lines the gene SLC16A1 encoding the protein MCT1 was the most enriched transcript. These data showed that glycolytic breast cancer tumors and cell lines exhibit a gene expression signature consistent with the Warburg effect, and that MCT1 may contribute to this glycolytic metabolism.

MCT1-4 are known to mediate proton-linked bi-directional transport of monocarboxylates such as lactate, pyruvate, and ketone bodies across the plasma membrane, and are thought to be crucial for adaptation to upregulated glycolysis (Halestrap and Meredith, 2004, Eilersten et al., 2014). MCT2 and MCT3 role in cancer are less studied, however MCT1 and MCT4 have been found to be most commonly upregulated in cancers (Halestrap and Wilson, 2012). Surprisingly we found that when we analyzed the mRNA levels of MCT1-4 in the breast tumors and cell lines, only MCT1 consistently strongly correlated with the glycolytic phenotype.

Further, we found that MCT1 protein expression was elevated in both lung and breast primary tissue, which is consistent with previous findings that have identified MCT1 upregulation in an array of primary human tumors, such as colon (Pinheiro et al., 2008), breast (Pinheiro et al., 2011), head and neck (Curry et al., 2013), and lung cancer (Izumi et al., 2011). Additionally, this elevation in MCT1 expression was associated with worse prognosis in patients.

Finally, we found that serum lactate and pyruvate levels were elevated in Stage IV lung cancer patients versus Stage I lung cancer patients, which is consistent with our previous results which shows enriched levels of MCT1 with increasing tumor malignancy. Despite the breast cancer patient serum samples (data not shown) not showing any significant difference between Stage IV and Stage I serum pyruvate or lactate levels, further study may be needed to determine whether measuring serum metabolite levels may be a potential prognostic tool.

In summary, our findings in chapter 1determined that MCT1 levels correlated with glycolytic metabolism and tumor malignancy in breast cancer patients.

MATERIALS AND METHODS

Enrichment Analysis

Gene expression data was analyzed using Gene set enrichment analysis (GSEA) (Subramanian et al., 2005) and Rank-rank hypergeometric overlap (RRHO) (Plaisier et al., 2010) algorithms as described previously (Palaskas et al., 2011). Pathway annotations for GSEA were from i) KEGG metabolic pathways (Kanehisa et al., 2010) or ii) the MSigDB curated gene sets (Subramanian et al., 2005). To visualize gene expression data within the context of metabolic pathway structure, we used Cytoscape (Smoot et al.) to color code the KEGG glycolysis pathway genes (hsa00010) on a green-to-red scale according to the average Pearson correlation with glycolytic phenotype.

Immunohistochemistry

Paraffin-embedded breast and lung cancer tissue microarray blocks were cut into 4 μm sections immediately prior to immunohistochemistry with polyclonal MCT1 antibody, and staining, blinded scoring, and statistical analyses were carried out as described previously (Mah et al., 2011; Mah et al., 2007; Yoon et al., 2010; Yoon et al., 2011). Comparisons of MCT1 expression across lung and breast histopathological categories were performed using Kruskal-Wallis tests, and the Cox proportional hazards model was used to determine prognostic values of survival.

Serum measurements

Blood samples were collected from patients in blood sample tubes and kept on ice until processing. Samples were spun at 1,800 x g for 10min. Supernatant was collected into 15ml centrifuge tubes and respun at 1,000 x g for 10min. Supernatant was collected as serum and frozen at -80°C until processing. Serum pyruvate and lactate levels were measured using an absorbance-based assay kit (BioVision).

References

Altenberg, B., & Greulich, K. O. (2004). Genes of glycolysis are ubiquitously overexpressed in 24 cancer classes. *Genomics*, *84*(6), 1014–20. doi:10.1016/j.ygeno.2004.08.010

Bensinger, S. J., & Christofk, H. R. (2012). New aspects of the Warburg effect in cancer cell biology. *Seminars in cell & developmental biology*, *23*(4), 352–61. doi:10.1016/j.semcdb.2012.02.003

Bonen, A., Miskovic, D., Tonouchi, M., Lemieux, K., Wilson, M.C., Marette, A., and Halestrap, A.P. (2000). Abundance and subcellular distribution of MCT1 and MCT4 in heart and fast-twitch skeletal muscles. American journal of physiology. Endocrinology and metabolism *278*, E1067-1077.

Chang, H.Y., Nuyten, D.S., Sneddon, J.B., Hastie, T., Tibshirani, R., Sorlie, T., Dai, H., He, Y.D., van't Veer, L.J., Bartelink, H., et al. (2005). Robustness, scalability, and integration of a wound-response gene expression signature in predicting breast cancer survival. Proc Natl Acad Sci U S A *102*, 3738-3743.

Chen, H., Wang, L., Beretov, J., Hao, J., Xiao, W., and Li, Y. (2010). Co-expression of CD147/EMMPRIN with monocarboxylate transporters and multiple drug resistance proteins is associated with epithelial ovarian cancer progression. Clin Exp Metastasis *27*, 557-569.

Curry, J. M., Whitaker-menezes, D., Ames, J. A., Anantharaman, A., Butera, A., Leiby, B., Cognetti, D. M., et al. (2013). MCT1 and MCT4 are functional biomarkers of metabolic symbiosis in head and neck cancer Cancer metabolism , stemness and tumor recurrence, 1371–1384.

Czernin, J., & Phelps, M. E. (2002). P OSITRON E MISSION T OMOGRAPHY S CANNING : Current and Future Applications, 89–112.

Eilertsen, M., Andersen, S., Al-Saad, S., Kiselev, Y., Donnem, T., Stenvold, H., Pettersen, I., et al. (2014). Monocarboxylate transporters 1-4 in NSCLC: MCT1 is an independent prognostic marker for survival. *PloS one*, *9*(9), e105038. doi:10.1371/journal.pone.0105038

Halestrap, A.P., and Meredith, D. (2004). The SLC16 gene family-from monocarboxylate transporters (MCTs) to aromatic amino acid transporters and beyond. Pflugers Arch *447*, 619-628.

Halestrap, A.P., and Wilson, M.C. (2012). The monocarboxylate transporter family--role and regulation. IUBMB Life *64*, 109-119.

Izumi, H., Takahashi, M., Uramoto, H., Nakayama, Y., Oyama, T., Wang, K.-Y., Sasaguri, Y., et al. (2011). Monocarboxylate transporters 1 and 4 are involved in the invasion activity of human lung cancer cells. Cancer science, 102(5), 1007–13. doi:10.1111/j.1349-7006.2011.01908.x

Kanehisa, M., Goto, S., Sato, Y., Kawashima, M., Furumichi, M., and Tanabe, M. (2014). Data, information, knowledge and principle: back to metabolism in KEGG. Nucleic Acids Res *42*, D199-205.

Kelloff, G. J., Hoffman, J. M., Johnson, B., Kelloff, G. J., Hoffman, J. M., Johnson, B., Scher, H. I., et al. (2005). Progress and Promise of FDG-PET Imaging for Cancer Patient Management and Oncologic Drug Development Management and Oncologic Drug Development, 2785–2808.

Mah, V., Marquez, D., Alavi, M., Maresh, E.L., Zhang, L., Yoon, N., Horvath, S., Bagryanova, L., Fishbein, M.C., Chia, D., et al. (2011). Expression levels of estrogen receptor beta in conjunction with aromatase predict survival in non-small cell lung cancer. Lung Cancer *74*, 318-325.

Mah, V., Seligson, D.B., Li, A., Marquez, D.C., Wistuba, II, Elshimali, Y., Fishbein, M.C., Chia, D., Pietras, R.J., and Goodglick, L. (2007). Aromatase expression predicts survival in women with early-stage non small cell lung cancer. Cancer Res *67*, 10484-10490.

McCleland, M.L., Adler, A.S., Deming, L., Cosino, E., Lee, L., Blackwood, E.M., Solon, M., Tao, J., Li, L., Shames, D., et al. (2013). Lactate dehydrogenase B is required for the growth of KRAS-dependent lung adenocarcinomas. Clin Cancer Res *19*, 773-784.

Neve, R.M., Chin, K., Fridlyand, J., Yeh, J., Baehner, F.L., Fevr, T., Clark, L., Bayani, N., Coppe, J.P., Tong, F., et al. (2006). A collection of breast cancer cell lines for the study of functionally distinct cancer subtypes. Cancer Cell *10*, 515-527.

Pinheiro, C., Albergaria, A., Paredes, J., Sousa, B., Dufloth, R., Vieira, D., Schmitt, F., and Baltazar, F. (2010). Monocarboxylate transporter 1 is up-regulated in basal-like breast carcinoma. Histopathology *56*, 860-867.

Pinheiro, C., Longatto-Filho, A., Scapulatempo, C., Ferreira, L., Martins, S., Pellerin, L., Rodrigues, M., Alves, V.A., Schmitt, F., and Baltazar, F. (2008). Increased expression of monocarboxylate transporters 1, 2, and 4 in colorectal carcinomas. Virchows Arch *452*, 139-146.

Pinheiro, C., Longatto-Filho, A., Simoes, K., Jacob, C.E., Bresciani, C.J., Zilberstein, B., Cecconello, I., Alves, V.A., Schmitt, F., and Baltazar, F. (2009). The prognostic value of CD147/EMMPRIN is associated with monocarboxylate transporter 1 co-expression in gastric cancer. Eur J Cancer *45*, 2418-2424.

Palaskas, N., Larson, S.M., Schultz, N., Komisopoulou, E., Wong, J., Rohle, D., Campos, C., Yannuzzi, N., Osborne, J.R., Linkov, I., et al. (2011). 18F-fluorodeoxy-glucose positron emission tomography marks MYC-overexpressing human basal-like breast cancers. Cancer Res *71*, 5164-5174.

Yoon, N.K., Maresh, E.L., Elshimali, Y., Li, A., Horvath, S., Seligson, D.B., Chia, D., and Goodglick, L. (2010). Elevated MED28 expression predicts poor outcome in women with breast cancer. BMC Cancer *10*, 335.

Yoon, N.K., Maresh, E.L., Shen, D., Elshimali, Y., Apple, S., Horvath, S., Mah, V., Bose, S., Chia, D., Chang, H.R., et al. (2011). Higher levels of GATA3 predict better survival in women with breast cancer. Hum Pathol *41*, 1794-1801.

Warburg, O. On the origin of cancer cells. *Science* **123**, 309–314 (1956)

Chapter 2

MCT1 inhibition reduces pyruvate but not lactate export, and enhances oxidative metabolism in glycolytic breast cancer cells

INTRODUCTION

Since glycolytic metabolism contributes to tumor growth in many cancers, efforts have been made to block tumor glycolysis. Presently, over 60% of tumors are recognized to be glycolytic and thereby presents a broad target that could affect many different types of cancers (Dakubo, 2010). One potential target is the family of monocarboxylate transporters (MCTs) that regulate cancer cell lactate export. The MCT family includes 14 members, but only MCT1-4 have been demonstrated to mediate proton-linked bi-directional transport of monocarboxylates such as lactate, pyruvate, and ketone bodies across the plasma membrane (Halestrap and Meredith, 2004). MCT levels and regulation plays an integral role in intracellular processes that balance the cell's homeostasis and its metabolic phenotype. For example, export of lactic acid prevents the decrease of cytosolic pH (pHi), and the inhibition of glycolysis. Tumor lactate export is thought to be primarily mediated by MCT1 and MCT4, since these are the family members most commonly upregulated in cancers (Halestrap and Meredith, 2004; Halestrap and Wilson, 2012). SLC16A1, the gene that encodes MCT1, was recently reported to be a MYC transcriptional target essential for lactate transport and glycolytic flux of certain cancer cell lines (Doherty et al., 2014). MCT1 levels also helps mediate pyruvate entry into the mitochondria for oxidative phosphorylation for ATP production (Halestrap et al., 2004). Furthermore, it has been suggested that MCT1 may play a role in communicating redox status between cells, as the lactate to pyruvate ratio also reflects the NAD+/NADH ratio in the cytosol (Poole et al., 1994). It has been shown that MCT1 inhibition induces cell death in Burkitt lymphoma cells and MCF7 breast cancer cells through disruption of lactate export, glycolysis and glutathione synthesis (Doherty et al., 2014). Consistent with this, small molecule inhibitors of MCT1 block activation of T cells reliant on increased glycolysis for proliferation through abrogation of lactate export (Guile et al.,

2006; Murray et al., 2005). These data together suggest that MCT1 is a viable target for cancer therapy. Currently an MCT1 inhibitor (AZD3965) is undergoing phase I evaluation in the United Kingdom for patients with solid tumors, prostate cancer, gastric cancer, and diffuse large cell B lymphoma (Polanski et al., 2014).

In this study we investigated the role of MCT1 in glycolytic metabolism. We investigated the change in glycolytic breast cancer cells metabolism upon loss of MCT1 function, and the role of MCT1 in regulating monocarboxylate transport.

RESULTS

Loss of MCT1 abrogates the similarity of glycolytic cells to tumors with high FDG update

In order to determine the role of MCT1 in the Warburg effect we generated breast cancer cell lines with short hairpin (sh)RNA-mediated stable knockdown of MCT1 (Figure 2-1). The cell lines used – HS578T, SUM149PT, and SUM159PT – are among the most glycolytic in our panel of 31 breast cancer cell lines (Figure 1-1). Using a threshold-free comparison of genome-wide expression patterns (Plaisier et al., 2010), we found that MCT1 knockdown in SUM149PT cells abrogated the similarity of these glycolytic cells to tumors with high FDG uptake (Figure 2-1.) Additionally, MCT1 knockdown results in altered expression of several nodes associated with highly glycolytic phenotypes, including HK1, PFKM. BPGM, and ENO1 (Figure 2-1). Treatment of HS578T cells for 24 hours with an MCT1 inhibitor (AZD3965) induced a gene expression signature that strongly resembles that of SUM149PT cells with stable MCT1 knockdown (Figure 2-2). Treatment of SUM149PT and SUM159PT cells with the MCT1 inhibitor abrogated the similarity to SUM149PT cells expressing scrambled shRNA.

Additionally, MCT1 inhibition decreased the similarity of these glycolytic cells to tumors with high FDG uptake (Figure 2-2). Together these data suggest that loss of MCT1 function changes gene expression of breast cancer cells to a less glycolytic phenotype.

MCT1 inhibition enriches genes involved in oxidative phosphorylation and oxygen consumption rates

Next, gene set enrichment analysis (GSEA) of MCT1 knockdown SUM149PT cells, as well as MCT1 inhibitor (AZD3965)-treated SUM149PT cells, showed enrichment in genes involved in oxidative phosphorylation, pyruvate metabolism, the TCA cycle, and, surprisingly, glycolysis (Figure 2-3). Enriched expression of oxidative phosphorylation genes was also observed upon MCT1 inhibition for 24 hours in additional breast cancer cell lines (Figure 2-4). Consistently, MCT1 inhibition results in increased oxygen consumption rates in multiple breast cancer cell lines after 24 hours treatment, but not after 0.5 or 4 hours AZD3965 treatment (Figure 2-4).

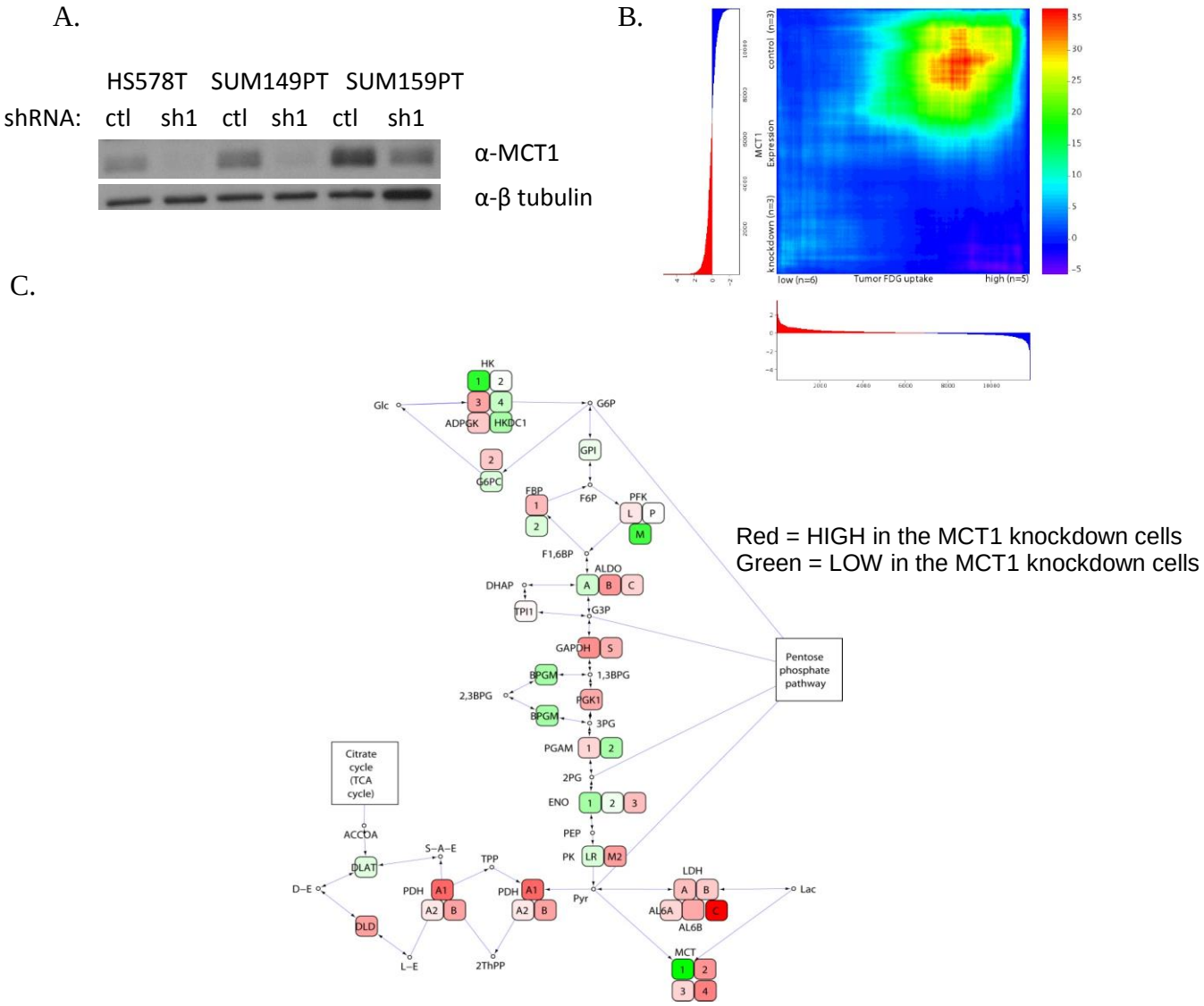

Figure 2-1. Cells with stable MCT1 knockdown exhibit altered expression of glycolytic genes. a, SUM159PT cells were infected with lentivirus containing the pLKO vector with scrambled shRNA or shRNA that knocks down MCT1 expression. After selection in puromycin for 5 days, mRNA was extracted and transcript levels were measured using an Affymetrix microarray. **b,** Gene expression profiles from SUM149PT cells expressing scrambled shRNA (control) and shRNA towards MCT1 (knockdown) were used to generate a ranked list of transcripts that are differentially expressed upon MCT1 knockdown. This ranked list was compared to a ranked list of transcripts that correlate with high FDG uptake in breast tumors from patients using the rank-rank hypergeometric overlap (RRHO) algorithm. The resulting overlap from the ranked lists, represented as a hypergeometric heat map, indicates that MCT1 knockdown renders glycolytic SUM149PT breast cancer cells less similar to tumors with high FDG uptake. The direction-signed $\log_{10}$-transformed hypergeometric p-values are indicated in the accompanying color scale. **c,** A comparison of glycolysis gene transcript levels in the MCT1 knockdown cells versus scrambled shRNA cells is depicted.

A.

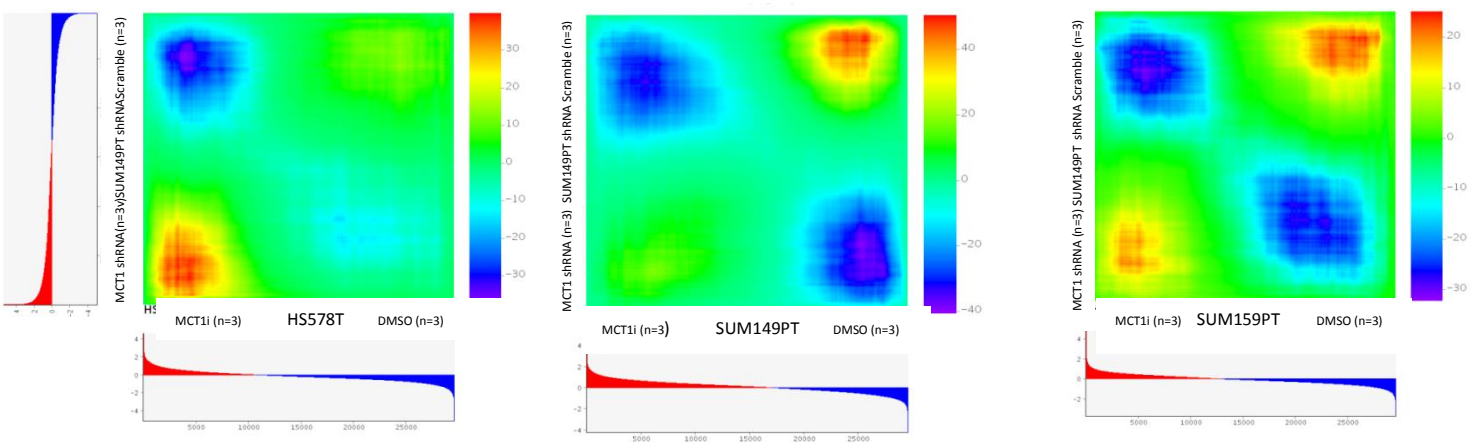

B.

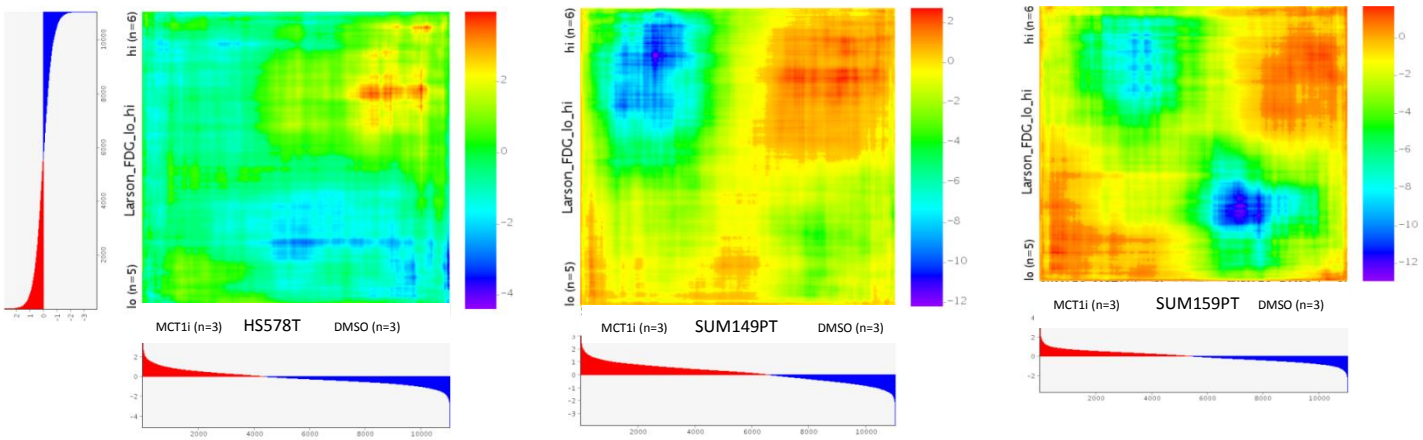

Figure 2-2. MCT1 inhibitor treatment induces a gene expression signature that resembles that of MCT1 knockdown and decreases similarity to breast tumors with high FDG uptake. mRNA was extracted from HS578T, SUM149PT, and SUM159PT cells treated for 24 hours with an MCT1 inhibitor (AZD3965) and transcript levels were measured using an Affymetrix microarray. These gene expression profiles were compared to mRNA from (a) SUM149PT cells expressing either scrambled (control) or MCT1 shRNA and (b) breast tumors with high or low FDG uptake by rank-rank hypergeometric analysis (Plaisier et al., 2010). The resulting hypergeometric heat maps indicate the degree of overlap between the two gene expression signatures where the direction-signed $\log_{10}$-transformed hypergeometric p-values are represented by the accompanying color scale. **a,** MCT1 inhibition rendered the gene expression profiles of HS578T cells more similar to SUM149PT cells with stable MCT1 knockdown. In SUM149PT and SUM159PT cells, MCT1 inhibition abrogated the similarity to SUM149PT cells expressing the scrambled shRNA. **b,** MCT1 inhibition rendered the gene expression profiles of all three glycolytic cell lines less similar to tumors with high FDG uptake.

A.

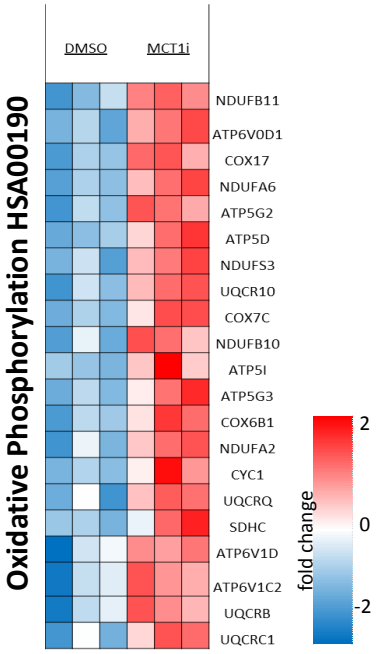

B.

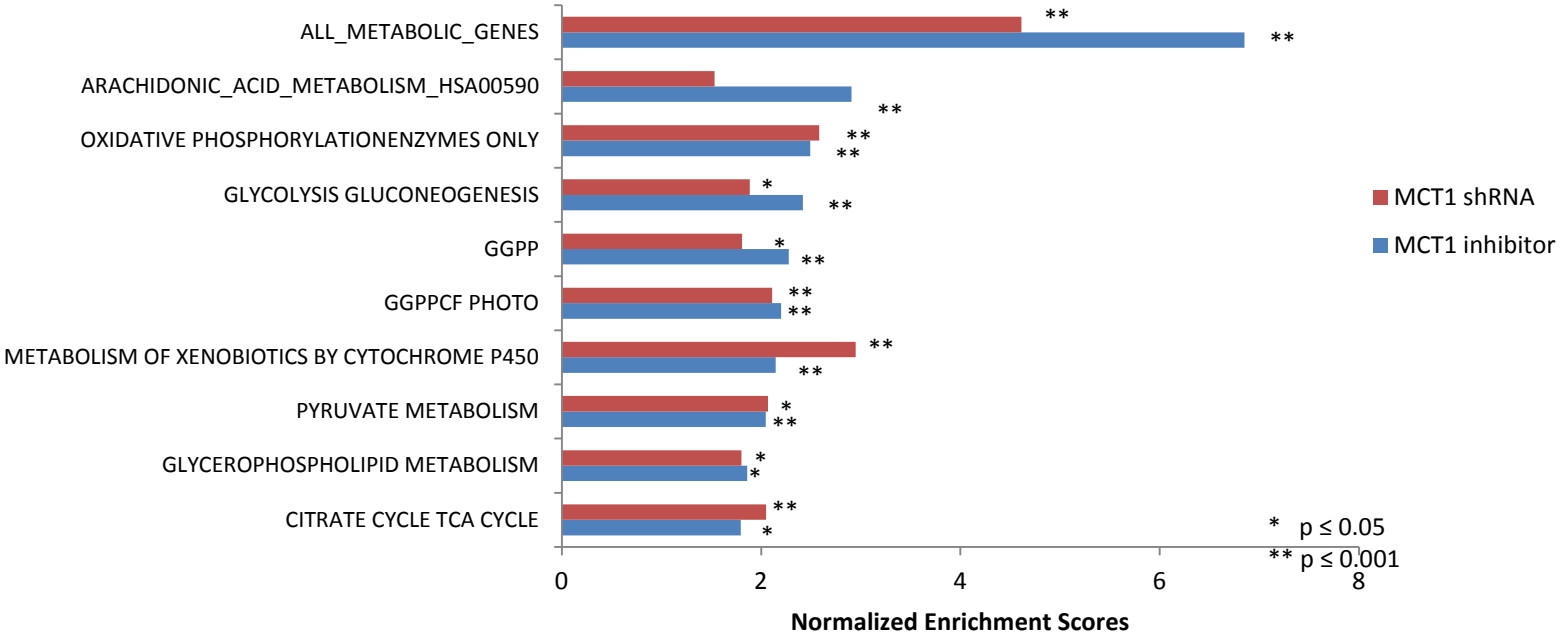

Figure 2-3. MCT1 knockdown and inhibition enriches the oxidative phosphorylation gene set in breast cancer cell lines. a, Heatmap indicating fold changes in expression levels of genes in the oxidative phosphorylation gene set from SUM149PT cells treated with DMSO or AZD3965 (MCT1i) for 24 hr. **b,** Gene set enrichment (GSEA) of MCT1 knockdown (red) SUM149PT cells, as well as MCT1i (AZD3965) (blue) treated SUM149PT cells, shows enrichment in oxidative phosphorylation enzymes, pyruvate metabolism and TCA cycle KEGG pathways.

A.

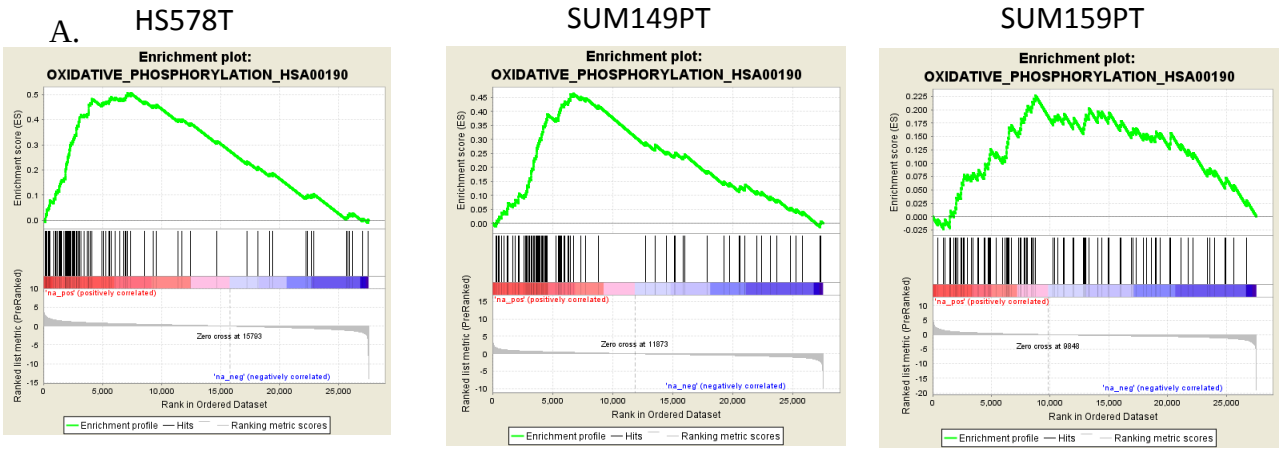

p –value < 0.001 for all three cell lines

B.

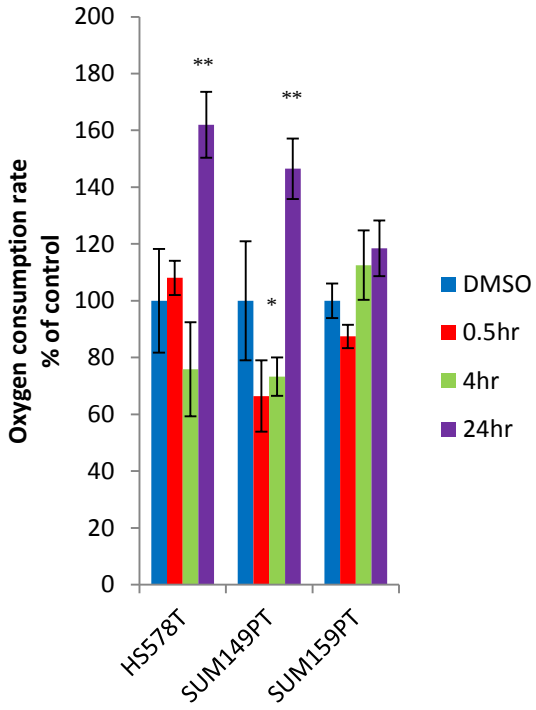

Figure 2-4. Acute MCT1 inhibition enriches the oxidative phosphorylation gene set and oxidative phosphorylation in breast cancer cell lines. a, HS578T, SUM149PT, SUM159PT were treated with vehicle (DMSO) versus 250 nM MCT1 inhibitor (AZD3965) for 24hrs. mRNA was extracted (Qiagen) and transcript levels were measured using Affymetrix (U133plus2.0). Mountain plots showing the enrichment of the oxidative phosphorylation gene sets in each of the cell lines is depicted. **b,** Cellular oxygen consumption rates post treatment with DMSO versus 250 nM AZD3965 (MCT1i).

MCT1 inhibition does not alter glycolytic flux or net lactate transport in glycolytic breast cancer cell lines

Notably however, lactate export rates and glucose uptake rates are not consistently altered upon MCT1 inhibition or MCT1 knockdown (Figure 2-5). Additionally, glycolytic flux as determined by conversion of 1,2-^{13}C-glucose to 1,2-^{13}C-lactate is also not consistently altered by MCT1 inhibition in breast cancer cell lines (Figure 2-6). These data suggest that MCT1 inhibition leads to enhanced oxidative metabolism in breast cancer cells through an alternative mechanism than reduced lactate export and disrupted glycolysis.

Next we measured the effect of MCT1 inhibition on lactate uptake in glycolytic breast cancer cells. To assess lactate uptake, 11 mM 1-^{13}C-lactate was added to the normal culture medium of SUM149PT cells along with 250 nM AZD3965 or DMSO, and 24 hours later, metabolites were extracted from the cells and media and analyzed by LC-MS/MS. AZD3965 treatment of SUM149PT cells had no effect on intracellular lactate levels, extracellular lactate levels, or percentage of ^{13}C-labeled intracellular lactate (Figure 2-7). The same experiment was conducted on SUM149PT cells cultured in media lacking glutamine, and while the percentage of ^{13}C-labeled intracellular lactate increased in the glutamine-deprived cells, MCT1 inhibition again had no effect on lactate levels or labeling (Figure 2-7). These results suggest that MCT1 does not impact lactate uptake in glycolytic breast cancer cells.

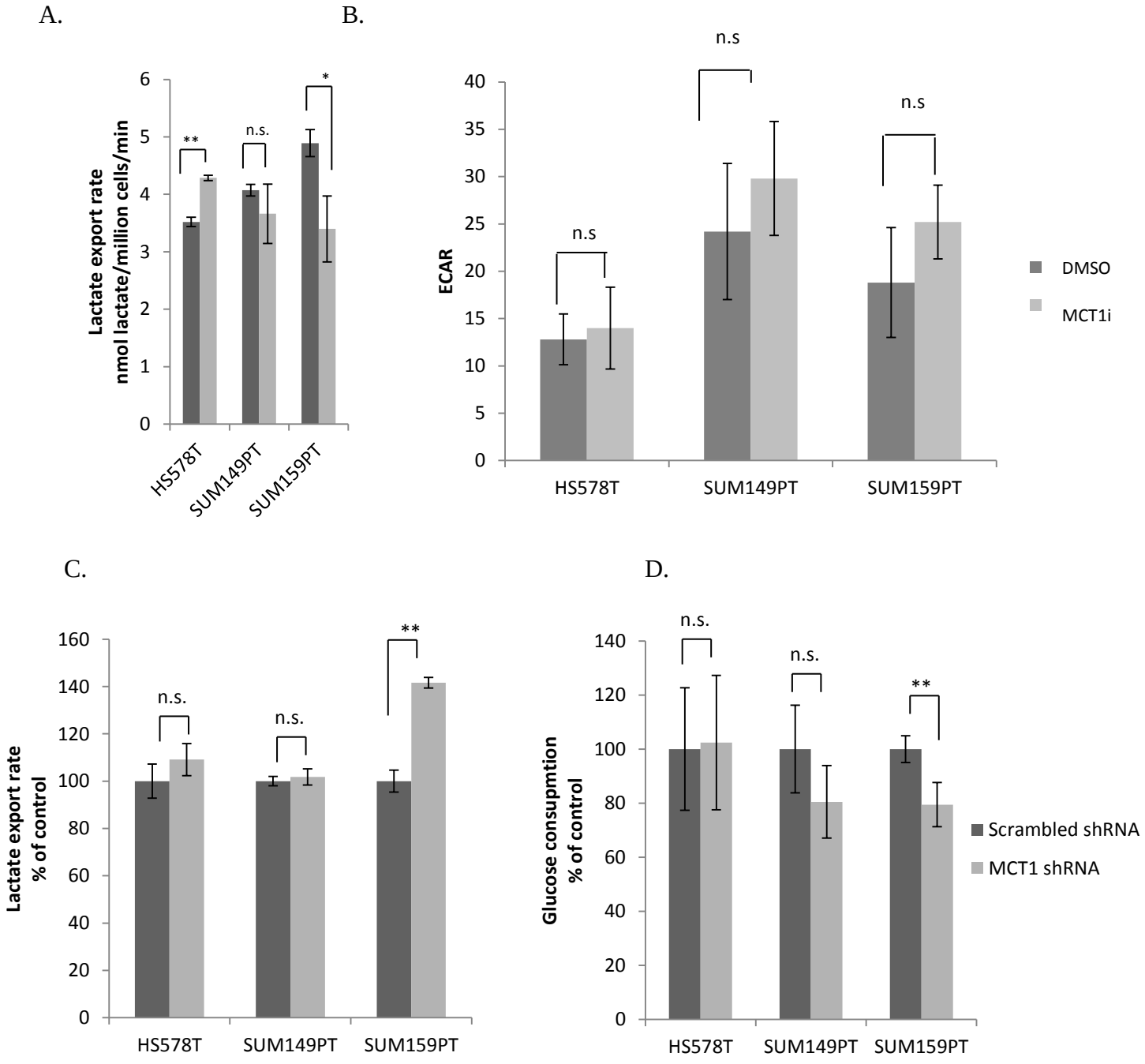

Figure 2-5. Lactate export rates, extracellular acidification and glucose uptake are not consistently altered upon MCT1 inhibition. a, Lactate export rates 4 hours post treatment of the indicated cell lines with DMSO or 250 nM AZD3965 (MCT1i). b**,** Extracellular acidification rates 24hrs post treatment with DMSO or 250nm AZD3965 (MCT1i). For **c-d** cells were infected with lentivirus containing the pLKO vector with scrambled shRNA or shRNA that knocks down MCT1 expression. Metabolic measurements were taken 5-7 days post knockdown (**c**), lactate export rates (**d**), glucose consumption rates (**d**). Error bars in c-**d** denote standard deviation (n=3). * denotes $p < 0.01$; ** denotes $p < 0.05$

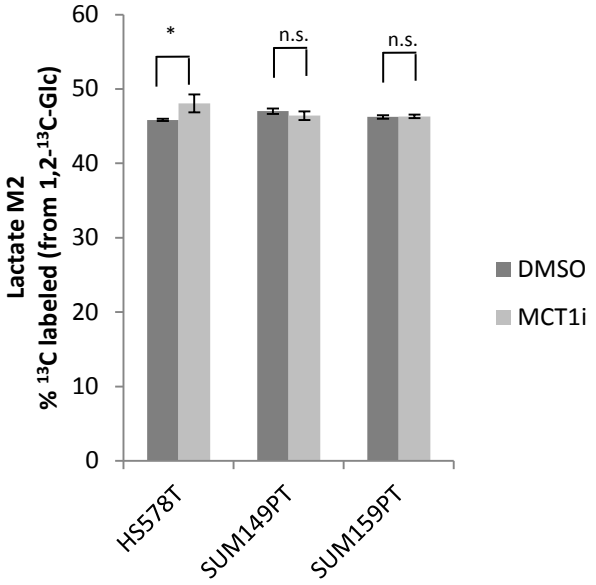

Figure 2-6. Glycolytic flux is not consistently altered upon MCT1 inhibition. Percentage of the ^{13}C-labeled M2 lactate isotopomer from cells 24 hr post labeling with 1,2-^{13}C-glucose and treatment with DMSO or 250 nM AZD3965 (MCT1i) as determined by LC-MS/MS.

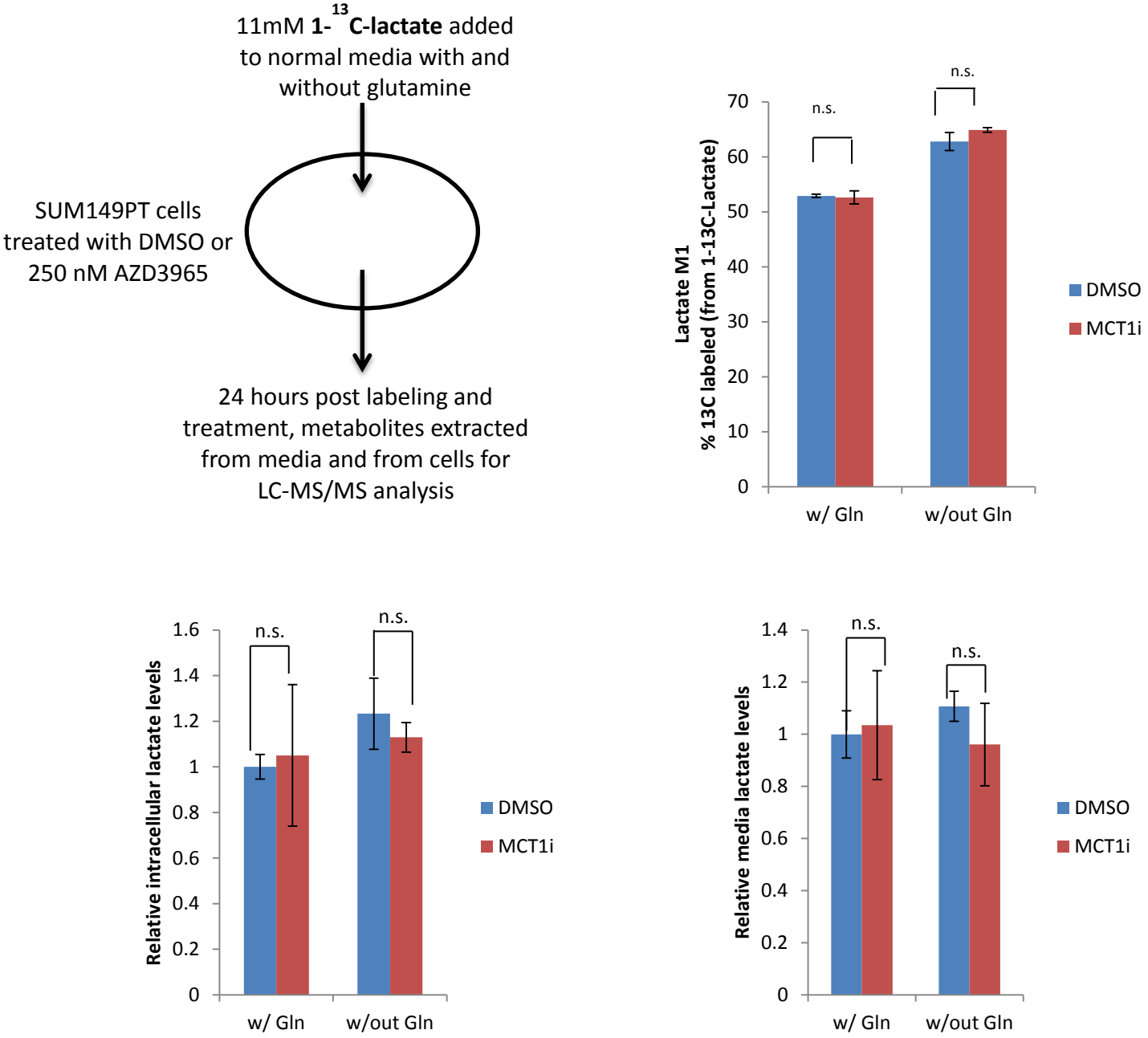

Figure 2-7. MCT1 inhibtion does not alter lactate uptake in SUM149PT cells. a, Schematic showing experimental setup. Briefly, 11mM 1-13C-lactate was added to normal culture media at the same time as addition of DMSO or 250nm AZD3965 (MCT1i). Metabolites were extracted from the cells and media 24 hrs post labeling and treatment, and analyzed by LC-MS/MS. **b,** Percentage of the ^{13}C-labeled M1 lactate isotopomer from cells 24 hr post labeling with 1-^{13}C-lactate and treatment with DMSO or 250 nM AZD3965 (MCT1i) in the presence or absence of 4 mM glutamine as determined by LC-MS/MS. **c,** Relative intracellular lactate levels as measured by LC-MS/MS. **d,** relative media lactate levels as measured by LC-MS/MS. Relative intracellular (**b**) and media (**c**) lactate levels were unchanged by treatment with AZD3965. For c and d, values shown are relative to lacate levels found in DMSO-treated cells grown in the presence of glutamine. Error bars in **b-d** denote standard deviation (n=3).

MCT1 inhibition reduces pyruvate export in glycolytic breast cancer cell lines

We next measured the effect of MCT1 inhibition on pyruvate export rates. As shown in Figure 2-8 all cell lines tested show decreased pyruvate export rates upon MCT1 inhibition with AZD3965, as well as increased intracellular pyruvate levels consistently in all cell lines, but not lactate levels (Figure 2-8).. Decreased pyruvate export rates were also observed upon stable MCT1 knockdown (Figure 2-8). Reduced pyruvate export rates were also observed using an alternative shRNA sequence that knocks down MCT1 expression (Figure 2-9), and expression of shRNA-resistant MCT1 cDNA rescued the reduced pyruvate export rate caused by MCT1 knockdown (Figure 2-10).

To better understand the role of MCT1 in regulating lactate versus pyruvate transport in breast cancer cells, we also measured lactate and pyruvate export rates over a time course post AZD3965-mediated MCT1 inhibition by analyzing metabolites extracted from the media via gas chromatography – mass spectrometry (GC-MS). We found that pyruvate media levels are reduced by acute MCT1 inhibition in SUM149PT cells, whereas lactate media levels are unchanged (Figure 2-11). Other breast cancer cell lines showed similar results (data not shown). Together these data confirm that MCT1 loss of function reduces cellular pyruvate export.

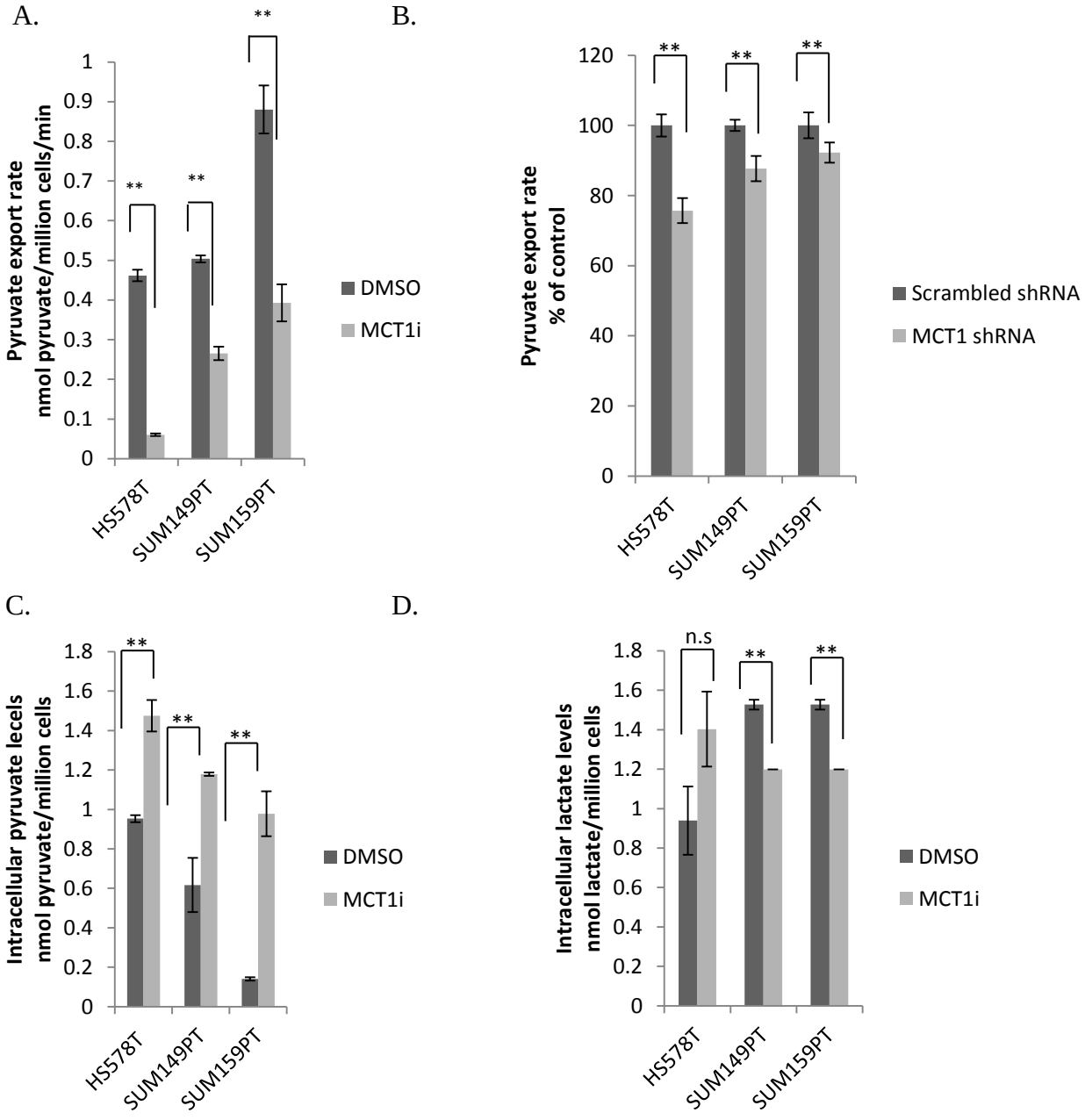

Figure 2-8. MCT1 is critical for pyruvate export in breast cancer cell lines. a, Pyruvate export rates 4 hours post treatment of the indicated cell lines with DMSO or 250 nM AZD3965 (MCT1i). **b,** Pyruvate export rates from cells that were infected with lentivirus containing the pLKO vector with scrambled shRNA or shRNA that knocks down MCT1 expression. Metabolic measurements were taken 5-7 days post knockdown. **c,** Intracellular pyruvate levels 30 minutes post treatement with DMSO or 250 nM AZD3965 (MCT1i). **d,** Intracellular lactate levels 30 minutes post treatement with DMSO or 250 nM AZD3965 (MCT1i).

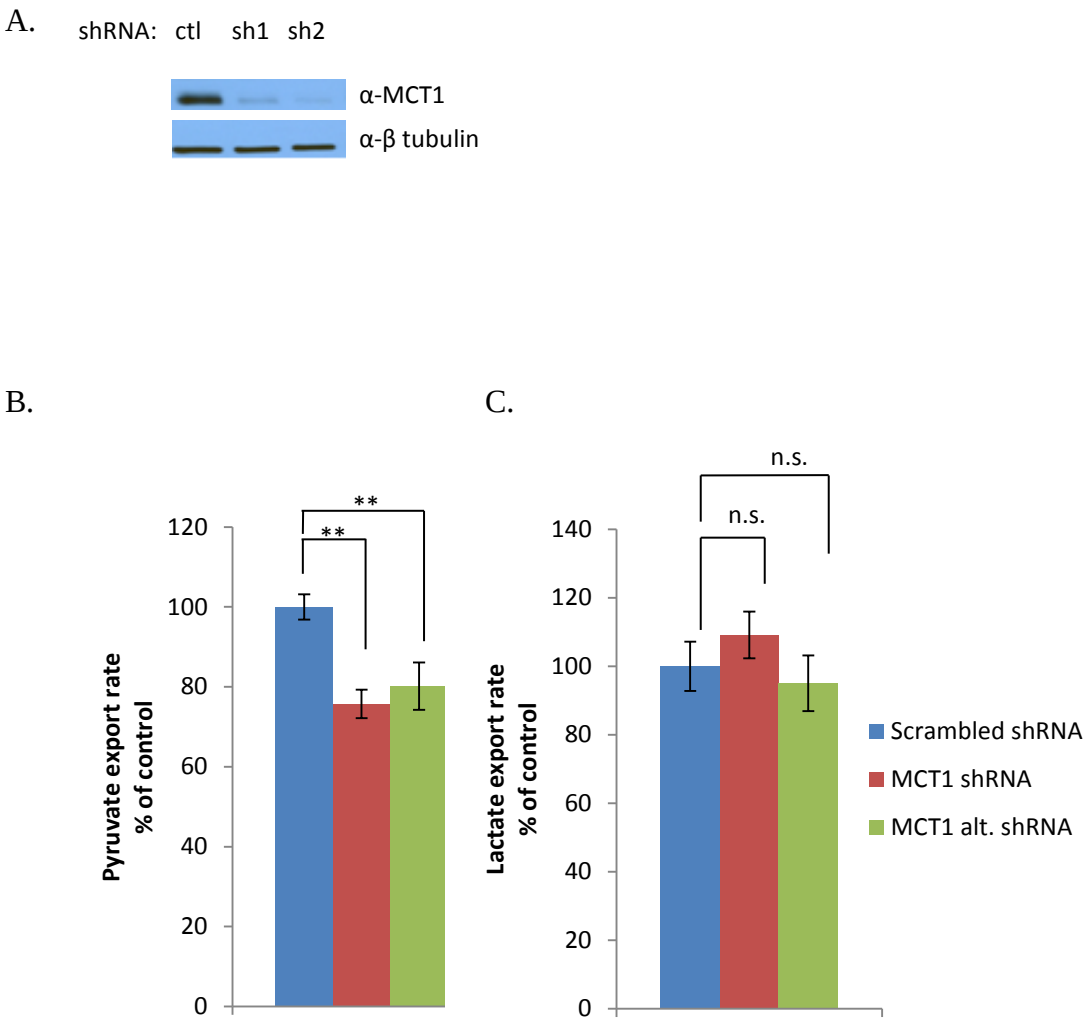

Figure 2-9. Alternate MCT1 shRNA also reduces pyruvate export and proliferation in breast cancer cells . a, Immunoblotting of the breast cancer cell line HS578T, stably expressing shRNA constructs. Cells were infected with lentivirus containing the pLKO vector with scrambled shRNA (cl) or shRNA that knocks down MCT1 expression (sh1) or an alternate shRNA that knocks down MCT1 expression (sh2). Metabolic measurements were taken 5-7 days post knockdown; blue bars indicate measurements from cells expressing scrambled shRNA, and red bars indicate measurements from cells expressing shRNA that knocks down MCT1 (sh1) and green bars indicate measurements from cells expression an alternate shRNA that knocks down MCT1 (sh2). **b-c, (b**), pyruvate export rates (**c**), and lactate export rates. Error bars in **b-c** denote standard deviation (n=3). * denotes $p < 0.01$; ** denotes $p < 0.05$

A.

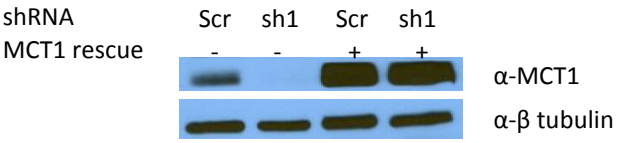

B.

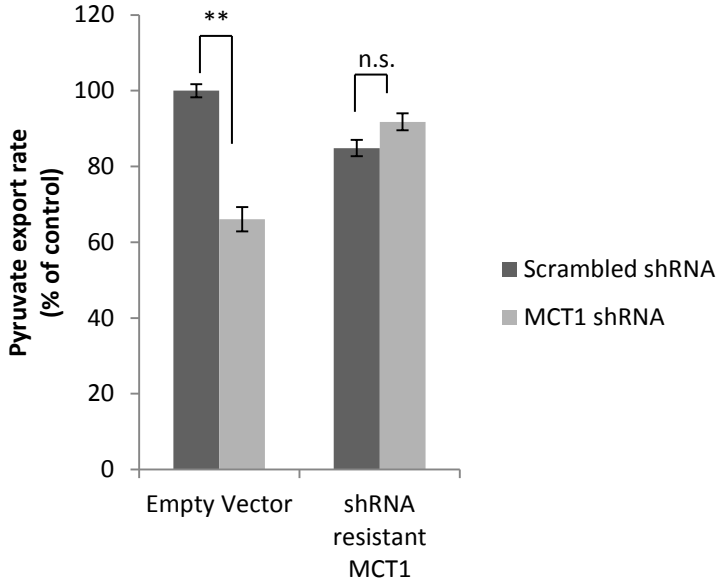

Figure 2-10. Overexpression of shRNA resistant MCT1 cDNA rescues MCT1 shRNA phenotypes in breast cancer cells. HS578T cells were infected with lentivirus containing the M4 vector or an M4 vector containing an MCT1 cDNA construct resistant to shRNA (MCT1 rescue), and selected for 5 days with blasticidin. Both cell lines were then infected with a lentivirus containing a pLKO vector with scrambled shRNA (Scramble shRNA) or shRNA that knocks down MCT1 expression (MCT1 kd shRNA) and selected with a media containing blasticidin and puromycin. **a,** Immunoblotting of the breast cancer cell line HS578T, stably expressing M4 or M4-MCT1 rescue and shRNA constructs. **(b)** Pyruvate export rates. Dark gray bars indicate measurements from cells expressing scrambled shRNA, and light gray bars indicate measurements from cells expressing shRNA that knocks down MCT1. Error bars denote standard deviation (n = 3).

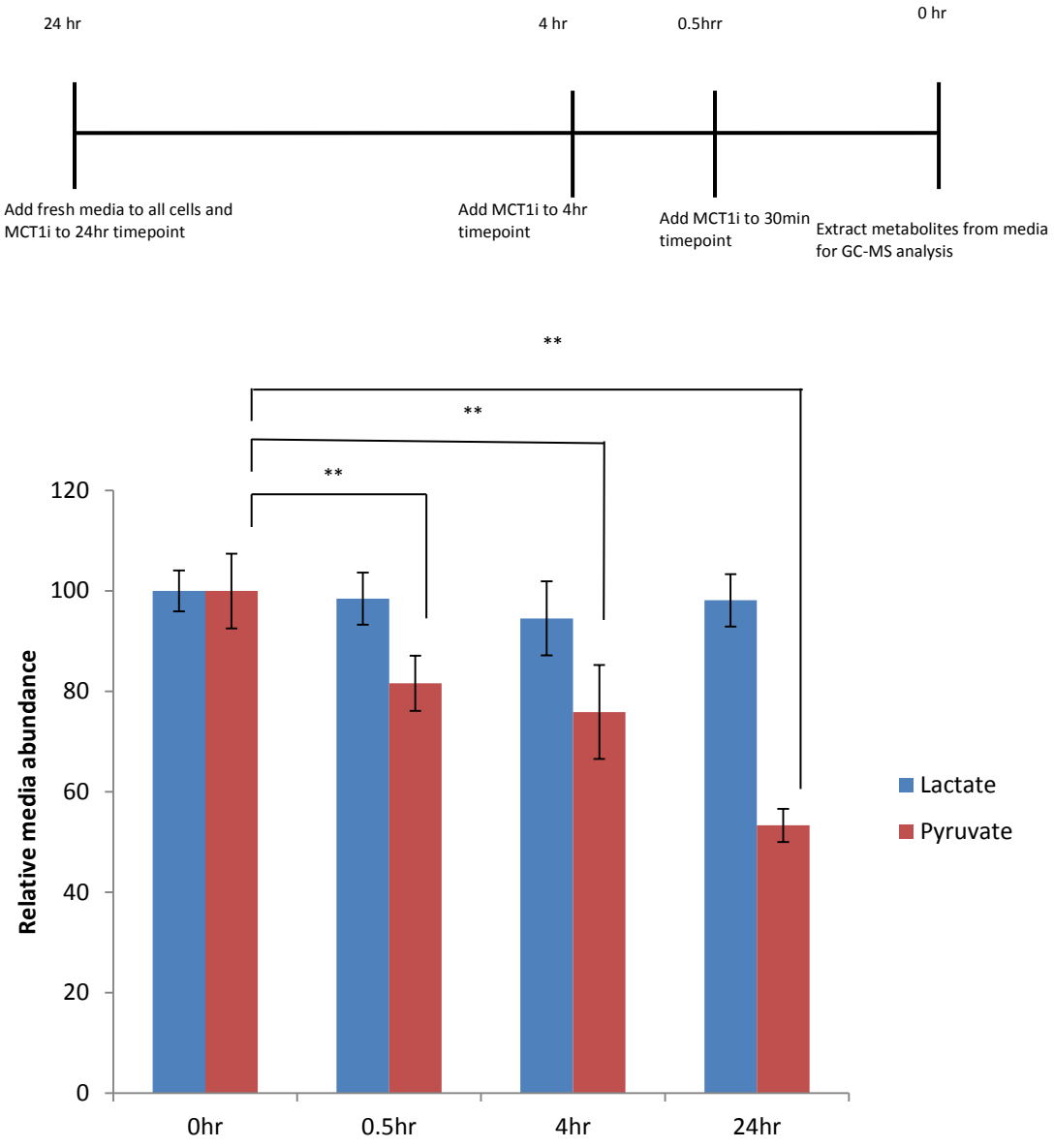

Figure 2-11. Acute MCT1 inhibition decreases for pyruvate export in breast cancer cell lines. Relative abundance of media lactate and pyruvate post treatment of SUM149PT cells with 250 nM AZD3965 (MCT1i) for the indicated times as determined by GC-MS. Error bars denote standard error of mean (n=5).

DISCUSSION

In the present study, we investigated the role of MCT1 in the Warburg effect in breast cancer cell lines.

We found that loss of MCT1 function in breast cancer cell lines altered the gene expression profiles of these cells to no longer resemble tumors with high FDG uptake, suggesting that the MCT1 inhibition caused the cells to take on a less glycolytic phenotype. To such, we found that knockdown and inhibition of MCT1 caused enrichment in oxidative phosphorylation genes, and an increase in oxidative phosphorylation at 24hrs MCT1 inhibition. However, further experiments found that loss of MCT1 function did not consistently alter lactate transport, nor glucose uptake, or glycolytic flux. Since the published K_m values for MCT1 interaction with pyruvate are lower than those for other monocarboxylates including lactate and acetate (K_m pyruvate = 0.6 - 1.0 mM versus K_m lactate = 2.2 - 4.5 mM, K_m acetate = 3.7)(Halestrap and Wilson, 2012), we hypothesized that MCT1 inhibition may affect pyruvate transport more than lactate transport in our cells. We determined that indeed, MCT1 inhibition caused a decreased in pyruvate export and an increase in intracellular pyruvate levels.

Doherty et al. recently found that MCT1 inhibition blocks lactate transport and decreases glycolysis to ultimately trigger cancer cell death in lymphoma and breast cancer cells (Doherty et al., 2014), however we did not observe reduced lactate export or decreased glycolysis upon MCT1 inhibition in glycolytic breast cancer cell lines. One potential explanation for these discrepancies is the varying levels of MCT4 in the different cell lines used. The Burkitt lymphoma cell lines and MCF7 and T47D breast cancer cell lines used in the study by Doherty et al. expressed very little, if any, MCT4. In contrast, the relatively more glycolytic breast cancer cell lines used in our study - SUM149PT, SUM159PT, and HS578T (Figure 1-1) -

expressed measurable amounts of MCT4 (Figure 3-10). MCT4 expression is likely responsible for continued lactate transport which likely sustains the glycolytic flux and survival of glycolytic breast cancer cell lines in the context of MCT1 inhibition.

The mechanism by which MCT1 inhibition leads to increased cellular respiration requires further investigation. Pyruvate export inhibition may lead to increased entry of pyruvate carbons into the mitochondria to provide more substrate for oxidative phosphorylation. However, our preliminary studies tracing the fate of ^{13}C-glucose metabolites, and specifically pyruvate, in MCT1-inhibited cells have yielded varying results across the breast cancer cell lines tested. Also, elevated oxygen consumption rates are observed at 24 hours post AZD3965 treatment, but not at 30 minutes or 4 hours post treatment (Figure 2-4), suggesting that the effect on respiration is not direct but rather through programmed changes in transcription. Consistent with this notion, genes involved in oxidative phosphorylation are enriched in breast cancer cells after 24 hours AZD3965 treatment (Figure 2-3). These changes in gene expression may occur through an unknown mechanism downstream of MCT1 inhibition and reduction of pyruvate export, or may simply be a cellular adaptation to survive MCT1 inhibition. It will be interesting to determine whether similar changes in gene expression also happen in tumors of breast cancer patients treated with AZD3965.

In summary our findings in chapter 2 determined that loss of MCT1 alters the glycolytic metabolism of our cells by enhancing oxidative metabolism independently from lactate transport or glycolysis. However, loss of MCT1 caused a reduction in pyruvate export suggesting that a primary function of MCT1 in glycolytic breast cancer cells may be to mediate pyruvate export.

MATERIALS AND METHODS

Cell culture

Human embryonic kidney 293T cells and HS578T breast cancer cells were maintained in Dulbecco's modified Eagle medium (DMEM) supplemented with 10% fetal bovine serum and 100U/ml of penicillin. SUM149PT and SUM159PT breast cancer cells were maintained in F12 medium and supplemented with 10% fetal bovine serum and 100U/ml penicillin, 10ug/ml insulin, 1ug/ml hydrocortisone, 10ng/ml EGF and 500ul of 50mg/ml gentamicin.

Cell lysis and immunoblotting

Breast cancer cells were lysed in buffer containing 50mM Tris, 150mM NaCl, 10mM beta-glycerophosphate, 1% NP-40, 0.25mM NaDeoxycholate, 10mM NaPP, 30mM NaF, 1mM EDTA, 1mM DTT, 1mM sodium orthovanadate, 4ug/ml of protease inhibitors aprotinin, leupeptin, and pepstatin. Western blot analysis was carried out according to standard protocols. The following antibodies were used:

shRNA constructs and lentiviral production

Five shRNA constructs targeting MCT1 were purchased from Sigma and were tested for their ability to knockdown expression of endogenous MCT1 (data not shown). The shRNA with highest MCT1 knockdown efficiency was used for infection of cell lines. A separate scramble shRNA was purchased from Sigma to use as a control. Lentivirus was made using a three plasmid packaging system as descrived previously (Root et al., 2006). Briefly, shRNAs in the pLKO.1-puro vector were cotransfected into 293T cells along with expression vectors containing the gag/pol, rev, and vsvg genes. Lentivrus was harvested 48hrs post transfection, and 5ug/mL polybrene was added.

Stable Cell Line Construction

For stable cell line construction, subconfluent breast cancer cell lines were infected with lentivirus containing scrambled or MCT1 shRNA, and cells were selected in 2 μg ml^{-1} puromycin for 5 days before experimentation.

Rescue construct and lentiviral production

Flag-tagged human MCT1 was cloned into a modified pCCL lentiviral vector (Thai et al., 2014). and were cotransfected into 293T cells along with expression vectors containing the gag/pol, rev, and vsvg genes. Lentivirus was harvested 36hrs post transfection, and 5ug/ml polybrene was added. Breast cancer cells were infected with harvested lentivirus, and selected in 10ug mL^{-1} blastocidin for two weeks.

Oxygen consumption

Oxygen Consumption rates were measured using two methods. An XF24 Analyzer (Seahorse Bioscience, North Billerica, MA, USA) was used to measure oxygen consumption on inhibitor treated cells [28]. The measurements were normalized against protein concentration. Data was obtained using the XF24 Analyzer software. Oxygen consumption rates of the stable cells were measured using an anaerobic chamber fitted with a polarographic oxygen electrode, and normalized against cell count[16]

Measurement of Glucose Consumption Rates and Pyruvate/Lactate Export Rates

Glucose consumption and lactate export rates were measured using a NOVA Bioanalyzer. Briefly, cells were seeded in triplicate in 10cm plates at 50% confluency. Twenty-four hours post

seeding the media was refreshed for all cells, and media added to an empty 10cm plate as a blank control. After 24hr incubation, 1ml of media was removed from each sample and the blank control and analyzed in the Nova BioProfile analyzer. Cell number was determined using a Coulter particle analyzer and used to normalize the calculated rates.

Pyruvate and lactate export rates and intracellular pyruvate and lactate levels were measured using an absorbance-based assay kit (BioVision) and GC-MS. Briefly, for the pyruvuate and lactate export rates cells were seeded in triplicate in 6 well plates at 50-70% confluency. Twenty-four post seeding, the media was removed and cells washed 2X with PBS. Cells were incubated for 4hrs in Krebs buffer. Aliquots from each well were assessed for amount of pyruvate and lactate present. Cell number was determined using a Coulter particle analyzer and used to normalize the calculated rates. To measure the intracellular pyruvate and lactate levels cells were seeded in triplicate in 10cm plates at 50-70% confluency. Tweny-four hours post seeding cells were treated with DMSO (ctl), MCT1i or methyl-lactate/pyruvate for 30min. Cells were lysed in NP40 lysis buffer and the lysates were spun in 10K filter columns for 10min at 4°C. Aliquots of the filtered lysate were assess for amount of pyruvate and lactate present.

Intracellular Metabolite Analysis Using LC-MS

Cells were carefully scraped off in 800 µL of 50% ice cold methanol. An internal standard of 10 nmol norvaline was added to the cell suspension, followed by 400 µL of cold chloroform. After vortexing for 15 min, the aqueous layer was transferred to a glass vial and the metabolites dried under vacuum. Metabolites were resuspended in 100 µL 70% acetonitrile (ACN) and 5 µL of this solution used for the mass spectrometer-based analysis. The analysis was performed on a Q Exactive (Thermo Scientific) in polarity-switching mode with positive voltage 3.0 kV and

negative voltage 2.25 kV. The mass spectrometer was coupled to an UltiMate 3000RSLC (Thermo Scientific) UHPLC system. Mobile phase A was 5 mM NH4AcO, pH 9.9, B) was ACN, and the separation achieved on a Luna 3μm NH2 100A (150 x 2.0 mm) (Phenomenex) column. The flow was 300 μL / min, and the gradient ran from 15% A to 95% A in 18 min, followed by an isocratic step for 9 min and re-equilibration for 7 min. Metabolites were detected and quantified as area under the curve (AUC) based on retention time and accurate mass (≤ 3 ppm) using the TraceFinder 3.1 (Thermo Scientific) software. Relative amounts of metabolites between various conditions, as well as percentage of labeling was calculated, corrected for naturally occurring ^{13}C abundance as described (Yuan et al., 2008), and depicted in bar graphs.

Cell Culture Medium Metabolite Analysis Using GC-MS

A total of 2.5 x 10^5 cells of each breast cancer cell line were seeded onto 6-well plates, medium was replaced after 24 hours and inhibitor added at appropriate times. Twenty microliters of cell-free medium samples were taken 24 hours thereafter. Metabolites were extracted by adding 300 μl 80% methanol to the medium samples, followed by vortexing 3X, then centrifugation for 10 minutes at 13k rpm at 4°C. The supernatant was transferred to a fresh tube, and the solvent was evaporated using a SpeedVac. Metabolites were derivatized by adding 20 μl of 2% methoxyamine hydrochloride in pyridine (Pierce) for 1.5h at 37 ºC followed by 30 μl N-methyl-N-(tert-butyldimethylsilyl)trifluoroacetamide (Pierce) for 1h at 55 ºC. Samples were run on an Agilent 5975C MSD coupled to an Agilent 7890A GC as described (Metallo et al.). Data extraction was done with Agilent MSD ChemStation software and analysis performed with Microsoft Excel. Metabolite isotopomers were not corrected for naturally occuring 13C.

References

G.D. Dakubo, Mitochondrial Genetics and Cancer, DOI 10.1007/978-3-642-11416-8_2, # Springer-Verlag Berlin Heidelberg 2010

Doherty, J.R., Yang, C., Scott, K.E., Cameron, M.D., Fallahi, M., Li, W., Hall, M.A., Amelio, A.L., Mishra, J.K., Li, F., et al. (2014). Blocking lactate export by inhibiting the Myc target MCT1 Disables glycolysis and glutathione synthesis. Cancer Res *74*, 908-920.

Guile, S.D., Bantick, J.R., Cheshire, D.R., Cooper, M.E., Davis, A.M., Donald, D.K., Evans, R., Eyssade, C., Ferguson, D.D., Hill, S., et al. (2006). Potent blockers of the monocarboxylate transporter MCT1: novel immunomodulatory compounds. Bioorg Med Chem Lett *16*, 2260-2265.

Halestrap, A.P., and Meredith, D. (2004). The SLC16 gene family-from monocarboxylate transporters (MCTs) to aromatic amino acid transporters and beyond. Pflugers Arch *447*, 619-628.

Halestrap, A.P., and Wilson, M.C. (2012). The monocarboxylate transporter family--role and regulation. IUBMB Life *64*, 109-119.

Murray, C.M., Hutchinson, R., Bantick, J.R., Belfield, G.P., Benjamin, A.D., Brazma, D., Bundick, R.V., Cook, I.D., Craggs, R.I., Edwards, S., et al. (2005). Monocarboxylate transporter MCT1 is a target for immunosuppression. Nat Chem Biol *1*, 371-376.

Polanski, R., Hodgkinson, C.L., Fusi, A., Nonaka, D., Priest, L., Kelly, P., Trapani, F., Bishop, P.W., White, A., Critchlow, S.E., et al. (2014). Activity of the monocarboxylate transporter 1 inhibitor AZD3965 in small cell lung cancer. Clin Cancer Res *20*, 926-937.

Poole RC, Halestrap AP (1993) Transport of lactate and other monocarboxylates across mammalian plasma membranes. Am J Physiol 264:C761–C782

Root, D. E., Hacohen, N., Hahn, W. C., Lander, E. S., & Sabatini, D. M. (2006). Genome-scale loss-of-function screening with a lentiviral RNAi library, *3*(9), 715–719. doi:10.1038/NMETH924

Chapter 3

MCT1 loss of function decreases breast cancer cell proliferation *in vitro* and tumor growth *in vivo*

INTRODUCTION

The Warburg Effect is characterized by increased metabolism of glucose to lactate even in the presence of oxygen (Warburg, 1956). Cancer cells as well as other rapidly proliferating cells, such as embryonic tissue (Xu et al., 2013) and activated T cells (Murray et al., 2005) are known to primarily rely on the Warburg effect for glucose metabolism. It is believed that proliferating cells adopt this altered metabolism in order to create biomass to fuel rapid proliferation (VanderHeiden et al., 2009).

The metabolic rewiring undergone in cells as they become cancerous has provided many novel targets for therapy (Galluzzi et al., 2013). Several inhibitors targeting glycolytic metabolism and other metabolic circuits are currently in Phase 1 clinical trials. AZD3965 (AstraZeneca) is a small molecule inhibitor that is currently undergoing Phase I trials in the UK for solid tumors. The inhibitor targets MCT1 which is known to be upregulated in many cancers (Halestrap and Wilson, 2012). Our own data has also shown that MCT1 may be a viable target by altering glycolytic metabolism by increasing oxidative phosphorylation, and therefore potentially affecting proliferation.

Retrospective epidemiology studies have also shown that whole-body metabolism can also affect risk of cancer development, cancer progression and response to therapy (Galluzzi et al., 2013). Studies have shown that treatment with metformin, a biguanide that is generally used to treat type II diabetes, may reduce cancer related mortality (Evans et al., 2005). Metformin and phenformin are known inhibitors of mitochondrial complex I and inhibit oxidative phosphorylation. Based on our data showing an increase in oxidative phosphorylation upon MCT1 inhibition, these biguanides could be used in conjunction with MCT1 to have an even bigger effect on proliferation of cancer cells.

In this study we investigated the effect of MCT1 in breast cancer cell proliferation *in vitro* and *in vivo*. Furthermore, we tested the synergistic effect of biguanides in dual treatment with MCT1 as a potential cancer therapy.

RESULTS

MCT1 loss of function decreases breast cancer cell proliferation *in vitro*

To examine whether MCT1 function affects breast cancer cell proliferation and survival, we measured the proliferation rates and viability of breast cancer cell lines stably expressing MCT1 shRNA or treated with AZD3965. MCT1 knockdown reduces glycolytic breast cancer cell proliferation (Figure 3-1, Figure 3-2), and this proliferative defect is rescued by expression of shRNA-resistant MCT1 cDNA (Figure 3-3). AZD3965 treatment also reduces proliferation rates of glycolytic breast cancer cell lines (Figure 3-1), and dose-response curves for AZD3965 indicate that the reduction in proliferation in glycolytic breast cancer cells tracks with the reduction in pyruvate export rate caused by MCT1 inhibition (Figure 3-4). Additionally, MCT1 knockdown increases the percentage of cells in the G0/G1 phase of the cell cycle (Figure 3-5). However, apoptosis-mediated cell death as measured by Annexin A5 staining is not affected by MCT1 knockdown in the breast cancer cell lines tested (Figure 3-6). These results suggest that MCT1 loss-of-function reduces proliferation of glycolytic breast cancer cells without enhancing apoptosis.

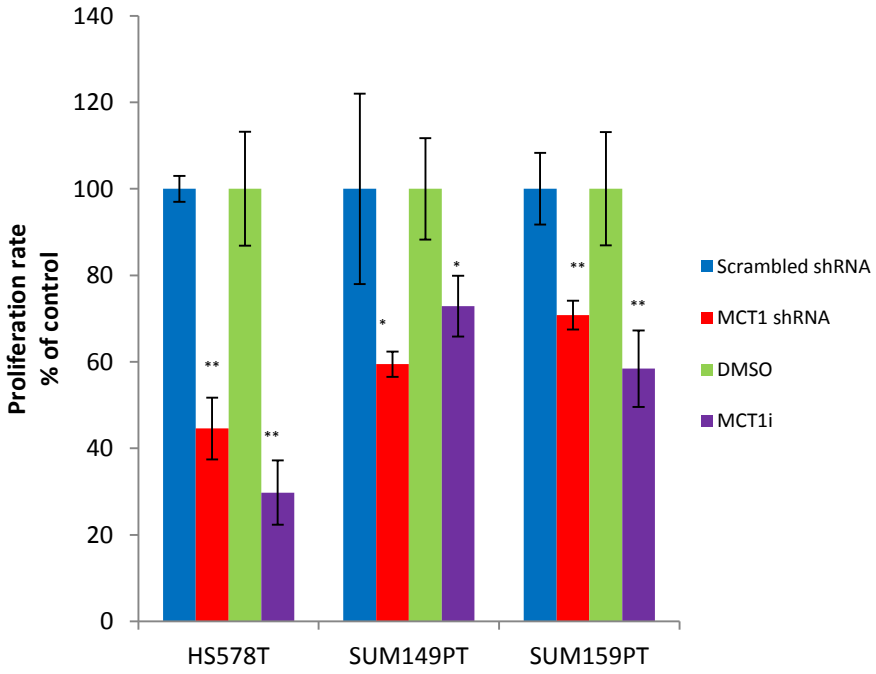

Figure 3-1. MCT1 loss-of-function reduces breast cancer cell proliferation. Proliferation rates of the indicated breast cancer cell lines stably expressing shRNA that knocks down MCT1 expression (MCT1 shRNA) versus control scrambled shRNA (scramble shRNA), and vehicle (DMSO) treated cells versus 250 nM AZD3965 (MCT1i).

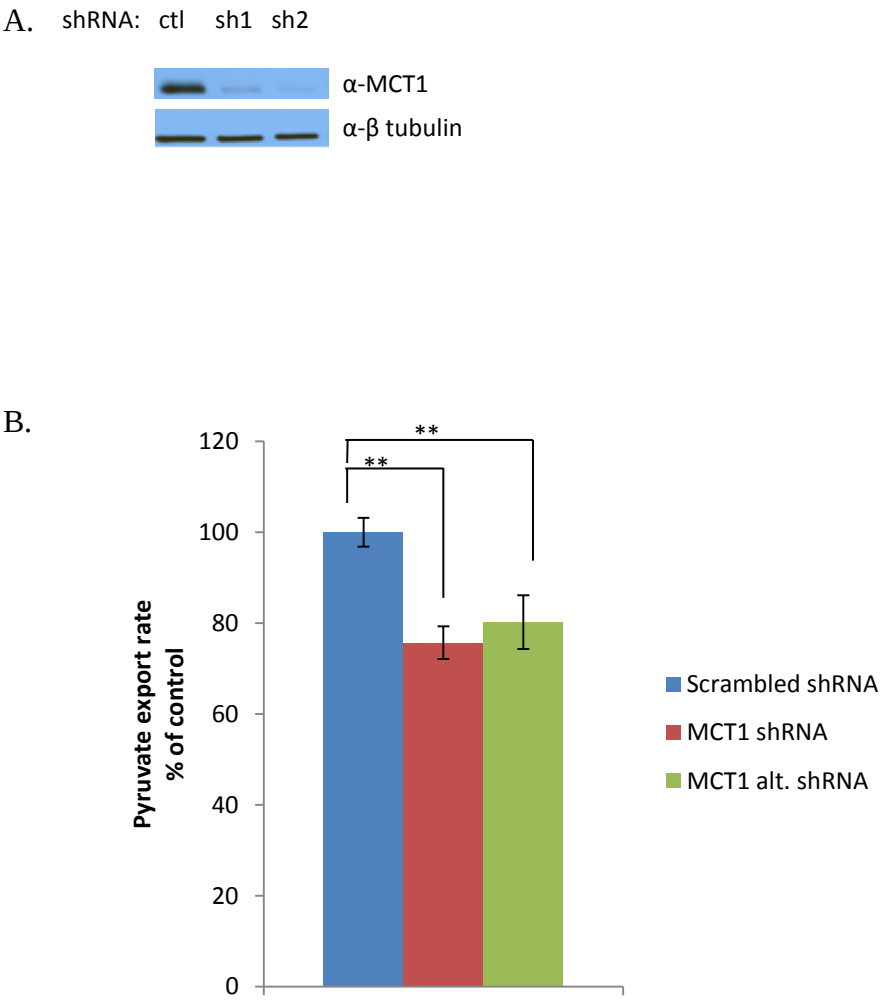

Figure 3-2. Alternate MCT1 shRNA reduces proliferation in breast cancer cells . a, Immunoblotting of the breast cancer cell line HS578T, stably expressing shRNA constructs. Cells were infected with lentivirus containing the pLKO vector with scrambled shRNA (cl) or shRNA that knocks down MCT1 expression (sh1) or an alternate shRNA that knocks down MCT1 expression (sh2). **(a)** Proliferation rates were measured by seeding cells on day 1, and counting cells on day 4. Metabolic measurements were taken 5-7 days post knockdown; blue bars indicate measurements from cells expressing scrambled shRNA, and red bars indicate measurements from cells expressing shRNA that knocks down MCT1 (sh1) and green bars indicate measurements from cells expression an alternate shRNA that knocks down MCT1 (sh2). Error bars in denote standard deviation (n=3). * denotes $p < 0.01$; ** denotes $p < 0.05$

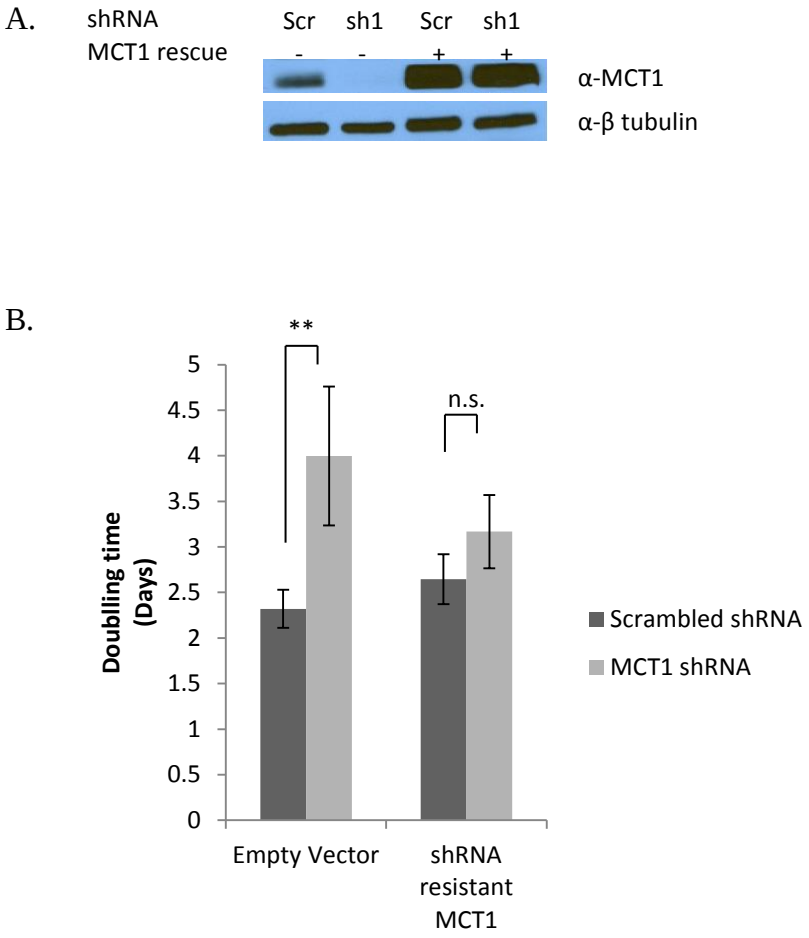

Figure 3-3. Overexpression of shRNA resistant MCT1 cDNA rescues MCT1 shRNA phenotypes in breast cancer cells. HS578T cells were infected with lentivirus containing the M4 vector or an M4 vector containing an MCT1 cDNA construct resistant to shRNA (MCT1 rescue), and selected for 5 days with blasticidin. Both cell lines were then infected with a lentivirus containing a pLKO vector with scrambled shRNA (Scramble shRNA) or shRNA that knocks down MCT1 expression (MCT1 kd shRNA) and selected with a media containing blasticidin and puromycin. **a,** Immunoblotting of the breast cancer cell line HS578T, stably expressing M4 or M4-MCT1 rescue and shRNA constructs. **(b)** Doubling time was determined by seeding cells on day 1, and counting cells on day 4, and calculating population doubling time. Dark gray bars indicate measurements from cells expressing scrambled shRNA, and light gray bars indicate measurements from cells expressing shRNA that knocks down MCT1. Error bars denote standard deviation (n = 3).

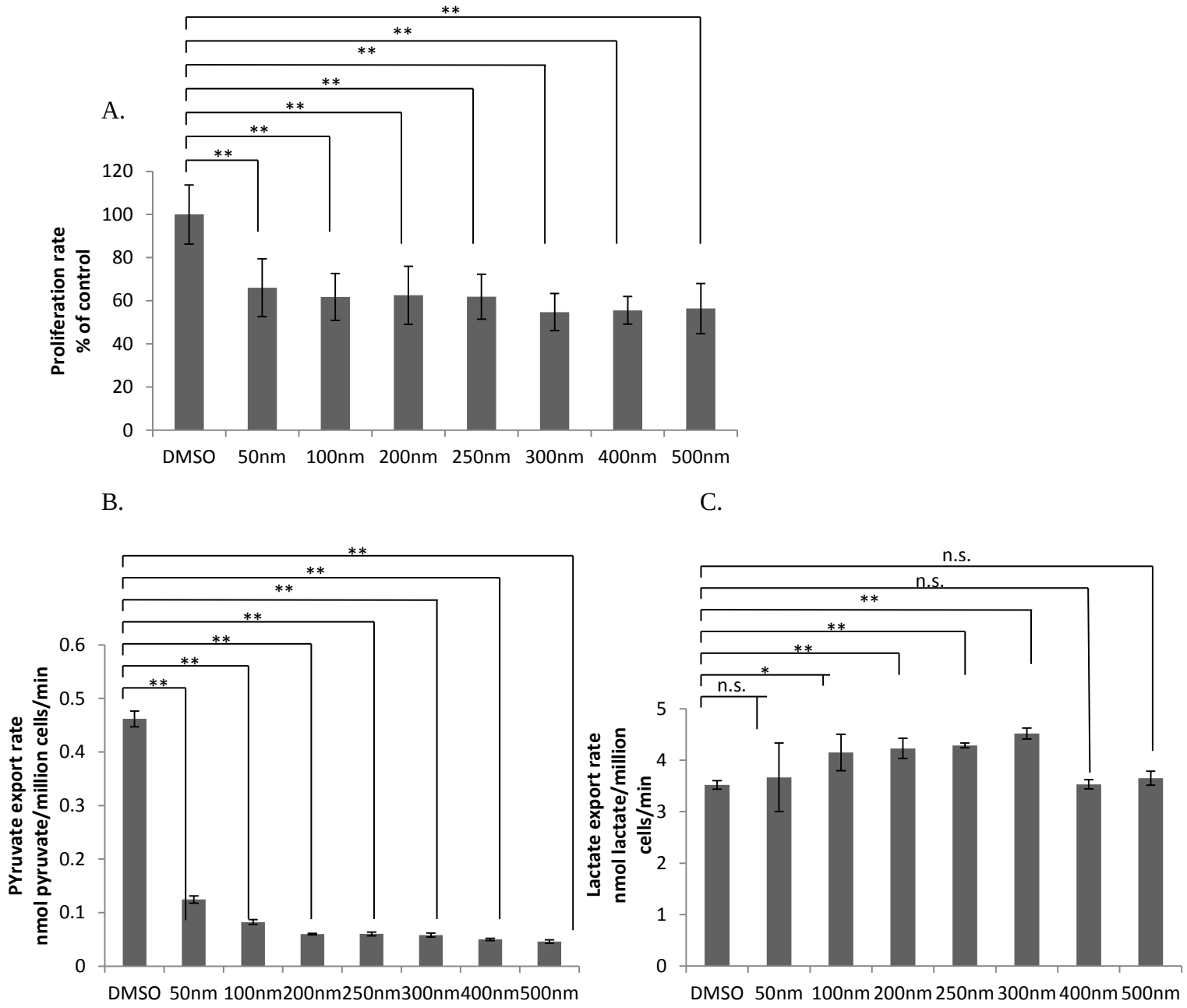

Figure 3-4. Pyruvate export and proliferation rates are reduced even at low concentrations of AZD3965. HS578T cells were treated with the indicated doses of AZD3965 or DMSO for 5 days cellular proliferation was measured. For a-**c**, HS578T cells were treated with indicated doses of AZD3965 for 4 hours, and pyruvate export, and lactate export rates were measured. a**,** AZD3965 dose response on proliferation rate of HS578T cells. b, AZD3965 dose response on pyruvate export rate of HS578T cells. c, AZD3965 dose response on lactate export rate of HS578T cells. Error bars in a denote standard deviation (n=6), and in b and c denote standard deviation (n=3). * denotes $p < 0.05$; ** denotes $p < 0.01$.

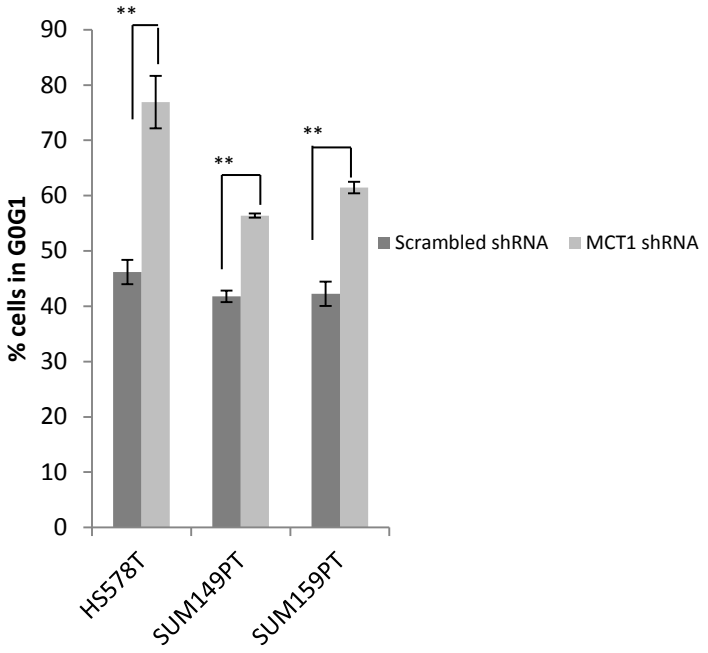

Figure 3-5. MCT1 loss-of-function increases halts cells in G0/G1 phase. Percentage of MCT1 knockdown cells (MCT1 shRNA) versus control cells (scramble shRNA) in the G0/G1 phase of the cell cycle.

A.

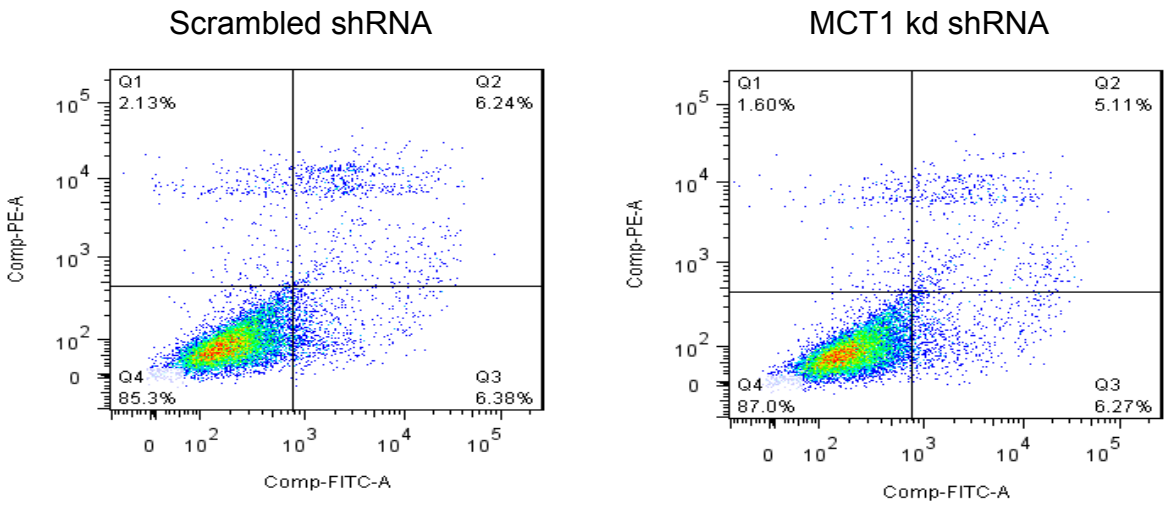

B.

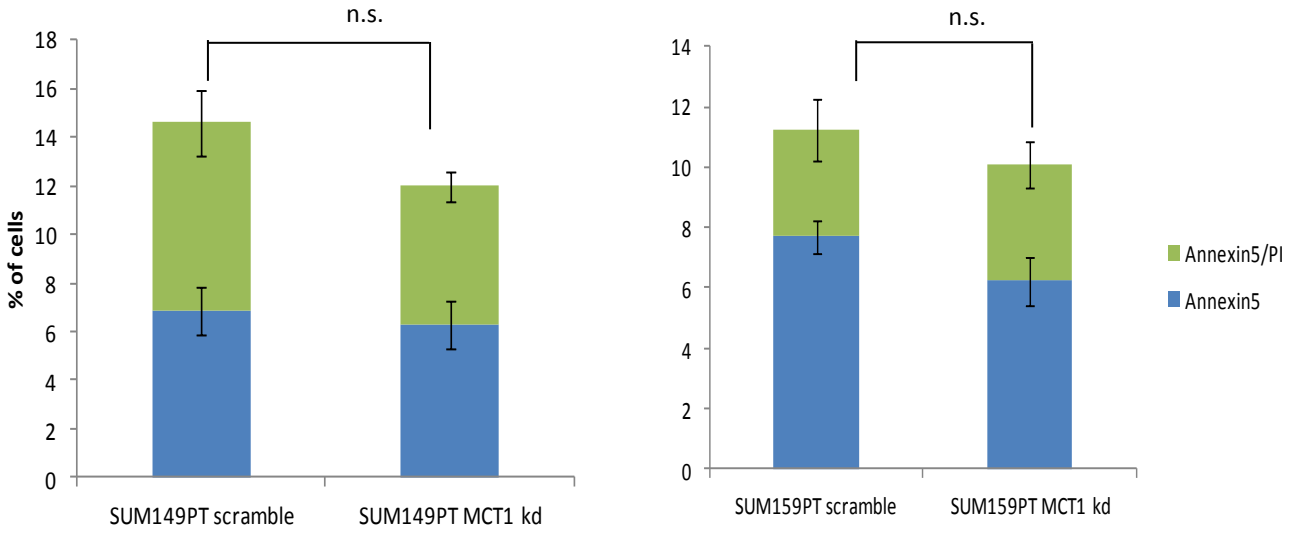

Figure 3-6. Cell viability is not affected by MCT1 knockdown. a,b, SUM149PT and SUM159PT cells were infected with lentivirus containing the pLKO vector with scrambled shRNA (Scramble shRNA) or shRNA that knocks down MCT1 expression (MCT1 kd shRNA). After 5 days of puromycin selection, 10^5 resistant cells were incubated with Annexin V and propidium iodide (PI) for 15 minutes and then analyzed by flow cytometry. **a,** Representative FACS plots showing percentage of cells in early apoptosis indicated by Annexin V positive, PI negative staining (lower right quadrant) and percentage of cell in late apoptosis marked by Annexin V/PI double positive staining (upper right quadrant). **b,** The number of early and late apoptotic cells is not affected by MCT1 knockdown in SUM149PT and SUM159PT cells. Percentage of early apoptotic cells are shown in blue, and percentage of late apoptotic cells are shown in green. Error bars denote standard deviation (n = 3).

Furthermore we investigated if increased intracellular pyruvate levels independent of MCT1 function would affect proliferation of the cells. We used plasma membrane permeable versions of lactate and pyruvate, methyl-lactate and methyl-pyruvate to increase the intracellular lactate and pyruvate levels in the cells. A concentration of 5mM methyl-pyruvate increased intracellular pyruvate levels similar to that of MCT1i, whereas 5mM of methyl-lactate did not increase intracellular lactate levels consistently in all the cell lines (Figure 3-7). We observed that treatment of the cells with 5mM methyl-pyruvate over a period of 5 days consistently caused a significant decrease in proliferation. Treatment with 5mM methyl-lactate did not show a consistent decrease in proliferation in all the cell lines (Figure 3-8).

The consistent reduction in proliferation rate upon MCT1 knockdown and AZD3965 treatment is surprising given that these cells express other MCTs (Figure 3-9), and MCT4 expression has been associated with resistance to MCT1 inhibition (Doherty et al., 2014; Le Floch et al., 2011; Polanski et al., 2014). MCT4 is expressed in the breast cancer cell lines tested with relatively high expression in SUM149PT and SUM159PT cells (Figure 3-9). The MCT1 shRNA sequences used in this study are not cognate to MCT2-4 mRNAs, and in fact SUM149PT cells with stable expression of MCT1 shRNA exhibit increased MCT2-4 transcript levels (Figure 2-1). However, MCT4 protein levels are not grossly altered in the context of MCT1 knockdown or inhibition in the breast cancer cell lines tested (Figure 3-10). Additionally, protein levels of the MCT chaperone protein CD147 are not altered in the context of MCT1 knockdown or inhibition in the breast cancer cell lines tested (Figure 3-10). Since we found that MCT1 loss-of-function reduces proliferation of glycolytic breast cancer cells that express other MCTs, including MCT4, our results suggest an important and specific role for MCT1 function in breast cancer cell proliferation.

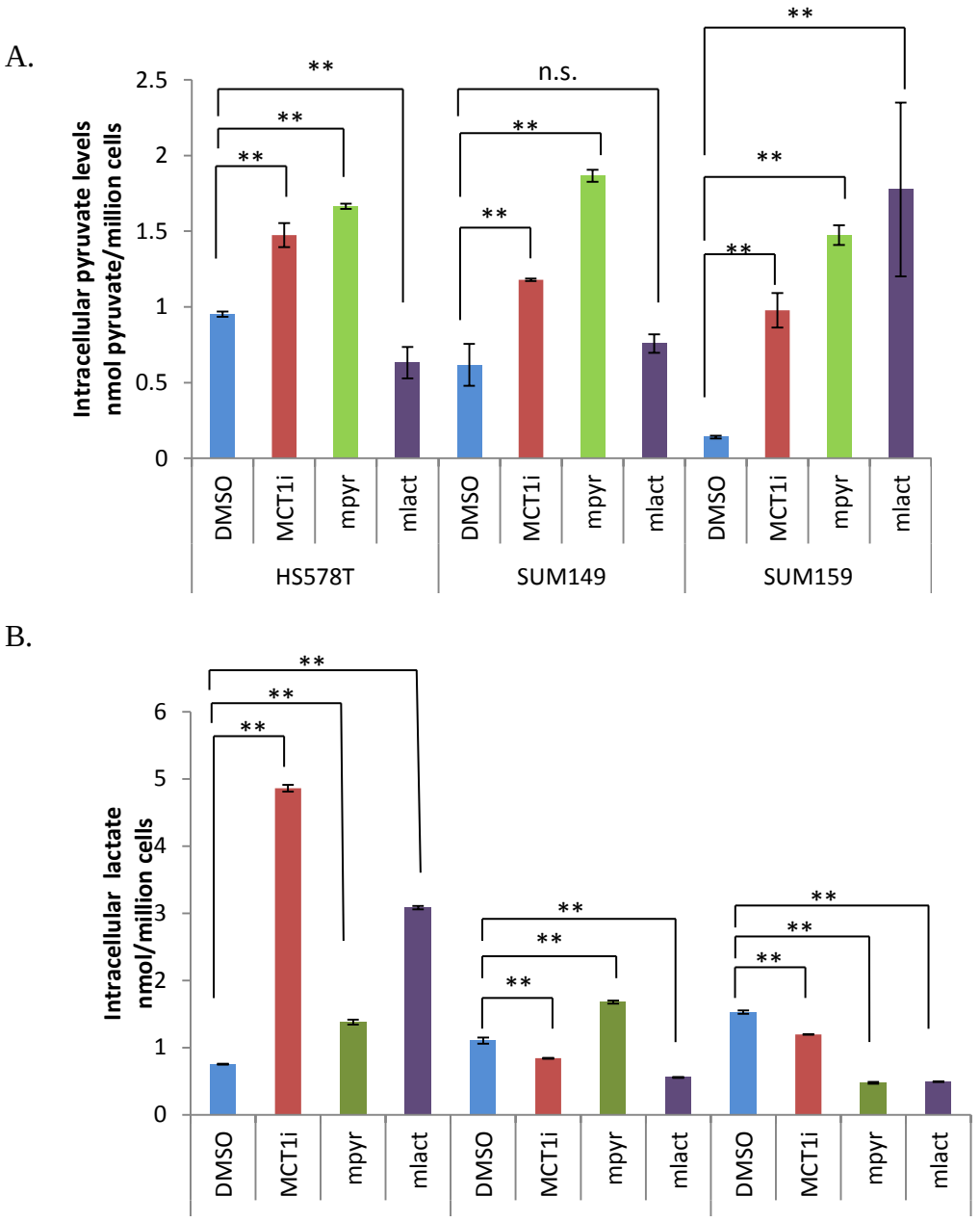

Figure 3-7. Methyl-pyruvate increases intracellular pyruvate levels in breast cancer cell lines. Cell lines were treated with DMSO, MCT1i, methyl-pyruvate or methyl-lactate for 30min, then lysed. Lysates were measured for intracellular carboxylate levels using a fluorescence based assay. **a,** Intracellular pyruvate levels. **b,** Intracellular lactate levels. Error bars denote standard deviation (n = 3).

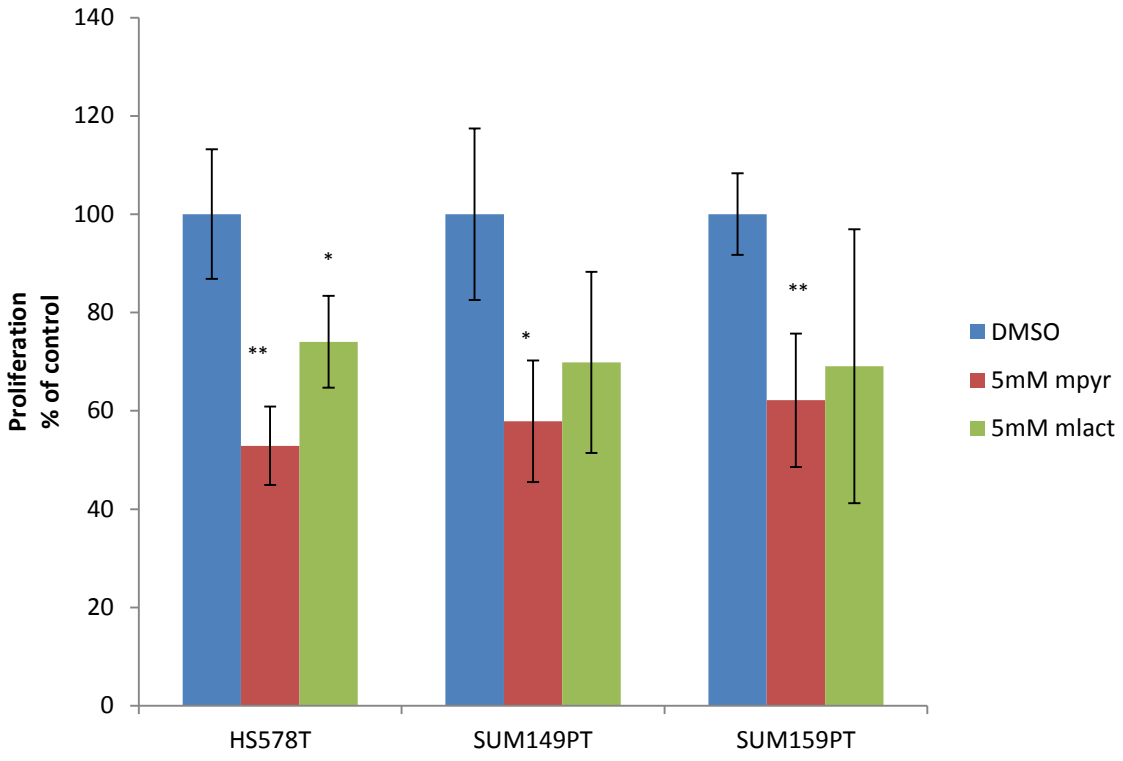

Figure 3-8. Methyl-pyruvate decreased proliferation of breast cancer cell lines. Cells were seeded on day 0 and counted on day 5. Cells were treated every day with DMSO, or methyl pyruvate or methyl lactate.

A.

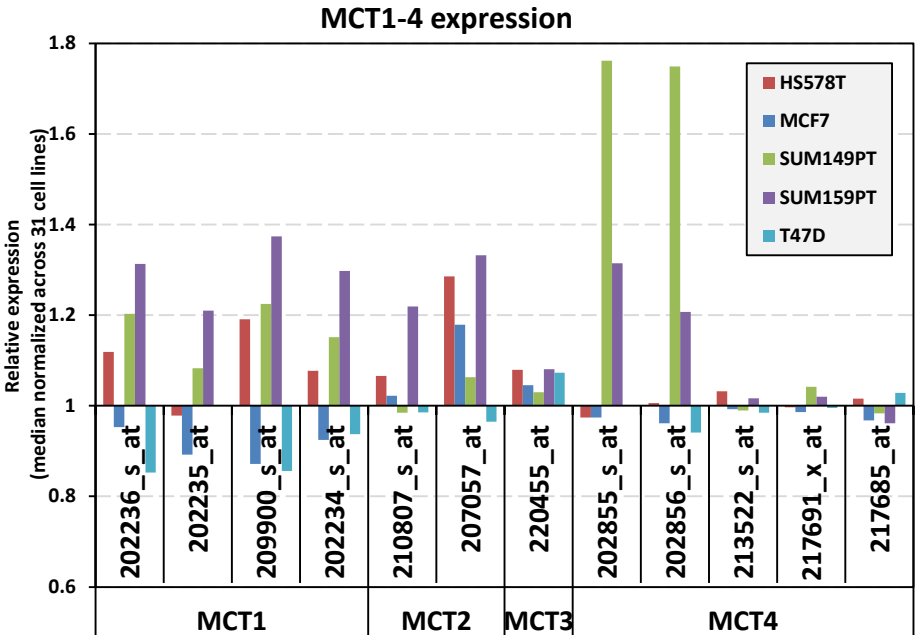

B.

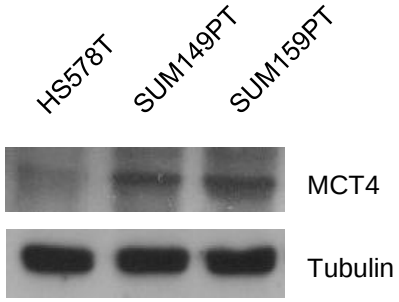

Figure 3-9. Breast cancer cells express other MCTs. a, MCT1-4 transcript levels determined by different microarray probes in HCC1937, HS578T, SUM149PT, and SUM159PT cells. **b,** Immunoblotting of whole cell lysates from the indicated breast cancer cell lines using antibodies towards MCT4 and tubulin. SUM149PT and SUM159PT cells express relatively higher amounts of MCT4.

A.

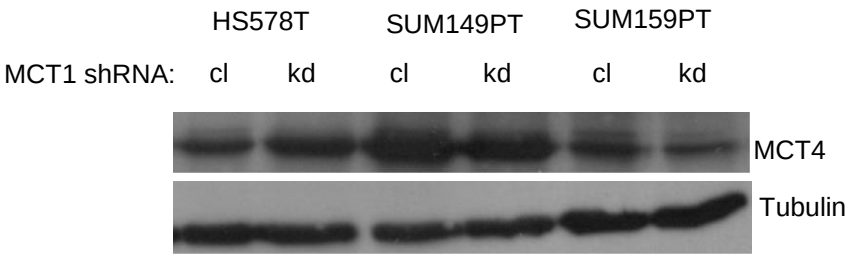

B.

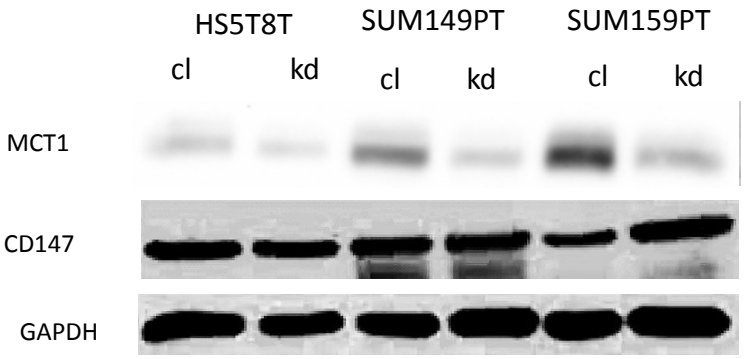

C.

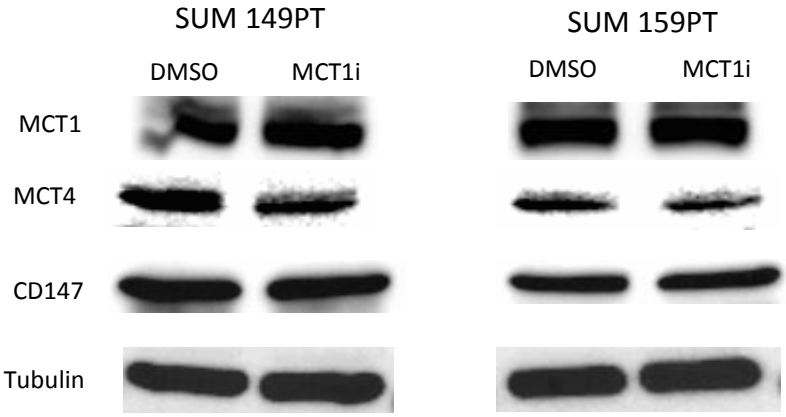

Figure 3-10. MCT4 and CD147 protein levels are not altered by MCT1 knockdown or inhibition in breast cancer cells. a, Immunoblotting of whole cell lysates from the indicated cell lines stably expressing scrambled shRNA (cl) or shRNA that knocks down MCT1 expression (kd). Whole cell lysates were probed with antibodies towards MCT4 and tubulin. MCT4 protein levels are reduced upon MCT1 knockdown in multiple cell lines including HCC1937 and HS578T cells. **b,** Immunoblotting of whole cell lysates from indicated breast cancer cell lines stably expressing scrambled shRNA (cl) or shRNA that knocks down MCT1 expression (kd). Whole cell lysates were probed with antibodies towards MCT1, CD147 and GAPDH. CD147 protein levels remain unchanged in HS578T and SUM149PT cells. SUM159PT cells express higher amounts of CD147 upon MCT1 knockdown. **c,** Immunoblotting of whole cell lysates from indicated breast cancer cell lines treated with DMSO or 250 nm AZD3965 (MCT1i) for 24hrs. Whole cell lysates were probed with antibodies towards MCT1, MCT4, CD147 and Tubulin. Levels of indicated proteins remain unchanged after MCT1i treatment.

MCT1 loss of function prevents tumor initiation *in vivo*

To examine whether loss of MCT1 impacts tumor initiation *in vivo*, we generated mammary fat pad xenograft tumors from SUM159PT cells with scramble shRNA knockdown and SUM159PT cells with MCT1 shRNA knockdown. The scramble cells were injected into the mice's right mammary fat pad, and the MCT1 knockdown cells into the mice's left mammary fat pad. The mice were checked twice a week for tumor growth, and measured by caliper upon tumor development. Tumor growth was observed on the right mammary fat pad of all the mice, whereas no tumors developed on the left mammary fat pads (Figure 3-11). These findings suggest that MCT1 may be necessary for tumor initiation for glycolytic breast cancer cells.

MCT1 inhibition decreases tumor growth *in vivo*

To examine whether MCT1 inhibition impacts tumor growth and glycolysis *in vivo*, we generated mammary fat pad xenograft tumors from SUM149PT cells in NOD scid gamma (NSG) mice, and began AZD3965 treatment after the tumors reached 5mm in diameter. AZD3965 treatment robustly blocked growth of the mammary fat pad xenograft tumors, with significant differences in tumor growth between the vehicle-treated and AZD3965-treated cohorts after only one week of treatment (Figure 3-12). However, despite the reduced tumor growth, tumor FDG uptake as measured by PET was not decreased in the AZD3965-treated mice, and instead was slightly but significantly increased (Figure 3-12). These data are consistent with our *in vitro* results showing that AZD3965 treatment reduces proliferation but not glycolytic flux of breast cancer cells.

Synergistic effects of MCT1 and biguanides further reduce glycolytic breast cancer cell proliferation

Since we found that MCT1 inhibition enhances oxidative metabolism, we reasoned that co-treatment of AZD3965 along with an oxidative phosphorylation inhibitor may synergistically reduce proliferation rates of glycolytic breast cancer cells. We therefore tested the effects of the biguanides, metformin and phenformin, known inhibitors of mitochondrial complex I, on glycolytic breast cancer cell proliferation in combination with AZD3965 treatment. Consistent with our hypothesis, dual treatment of AZD3965 with metformin or phenformin further lowered proliferation rates, beyond those seen with AZD3965 treatment alone, in an additive to synergistic fashion in multiple breast cancer cell lines (Figure 3-13). Similar synergistic effects between MCT1 inhibition and metformin treatment were recently reported in mouse xenograft models of cancer (Doherty et al., 2014). Collectively, these additive to synergistic effects of metformin or phenformin dual treatment with AZD3965 in cancer cell lines and tumors suggest a promising combination treatment strategy for patients with glycolytic tumors.

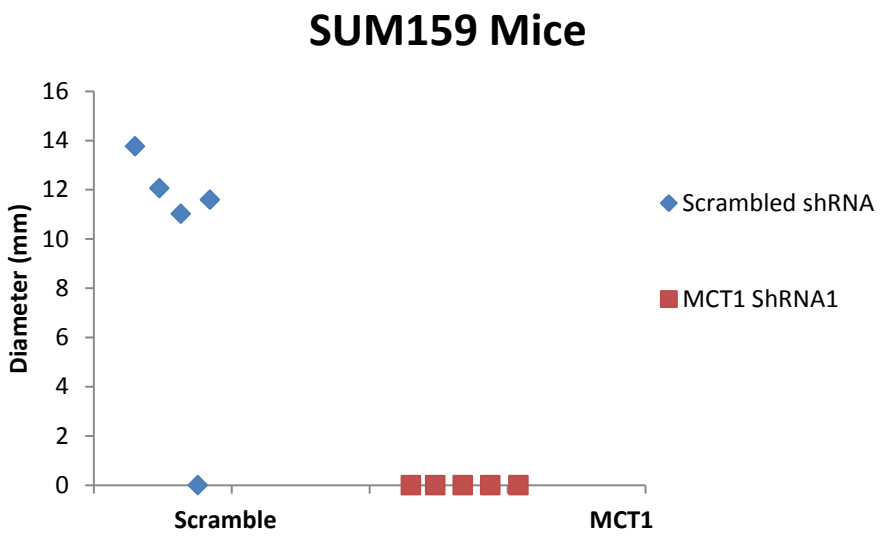

Figure 3-11. MCT1 loss-of-function prevents tumor initiation in SUM159PT cells. Size of mammary fat pad xenograft tumors in NSG mice. Tumors are derived from SUM159PT cells.

A.

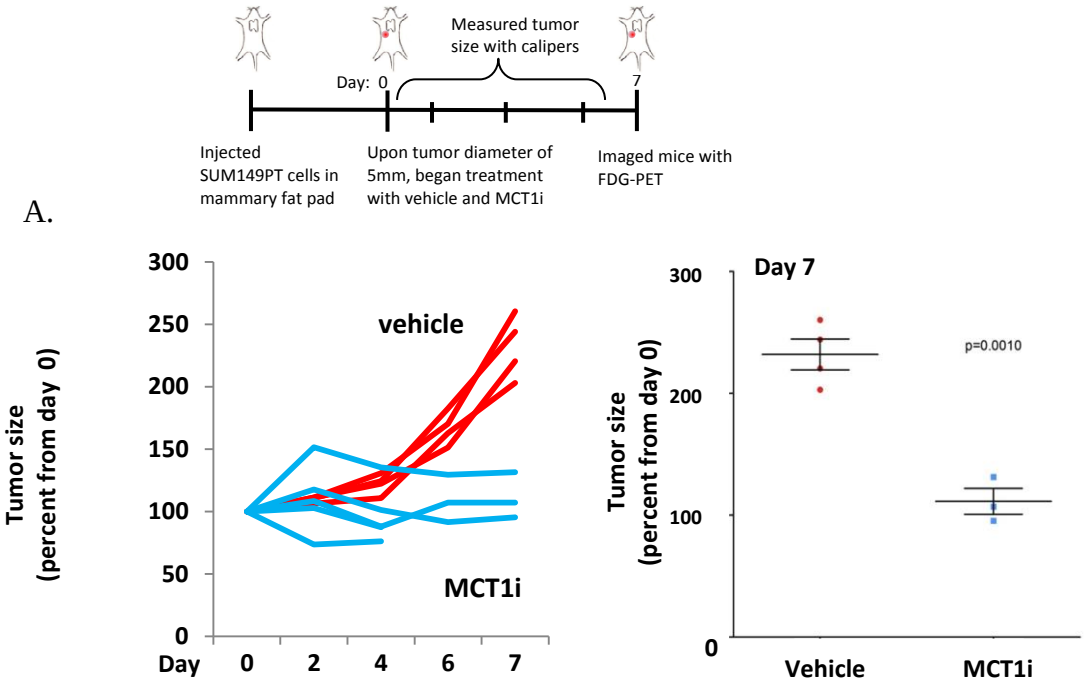

B.

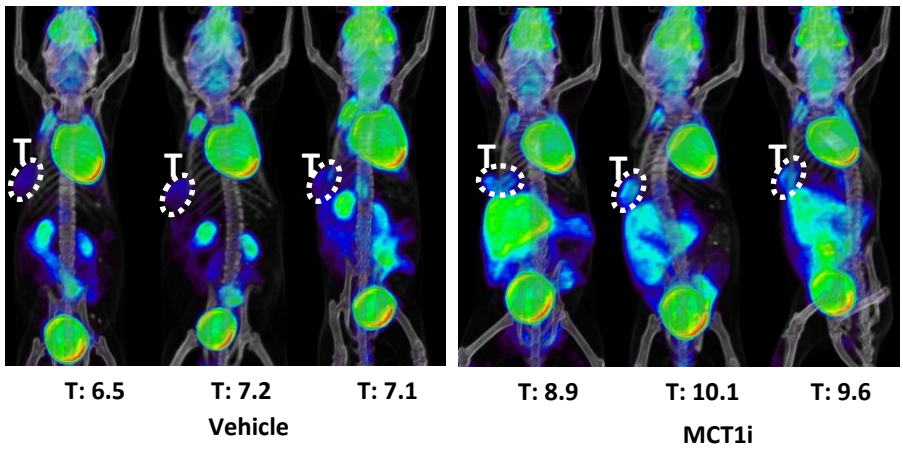

Figure 3-12. MCT1 loss-of-function suppresses tumor growth. a and b, Relative tumor volumes (**a**) and FDG-PET/CT images (**b**) from NSG mice with mammary fat pad xenograft tumors derived from SUM149PT cells treated by oral gavage twice daily with either 0.5% hydroxypropyl methyl cellulose/0.1%tween (vehicle) or 0.1ml/10g AZD3965 (MCT1i) for seven days. In (**b**) T indicates tumor, and values shown represent mean injected dose per gram (%ID/g) calculated from tumor regions of interest. Error bars denote standard deviation n=4.

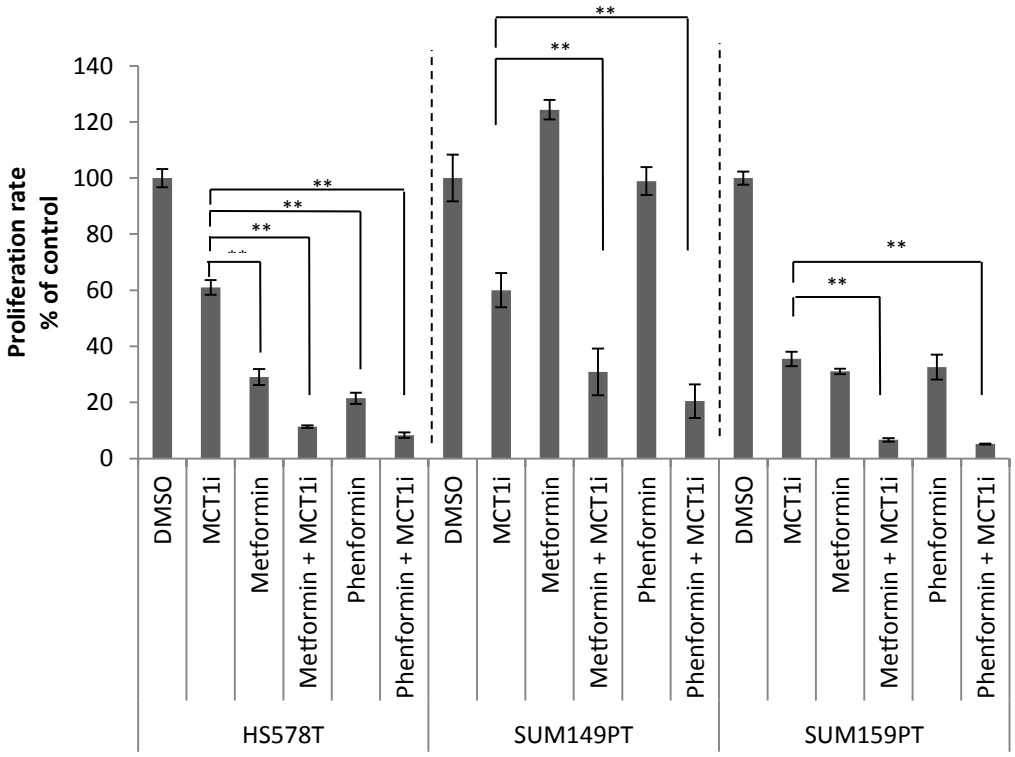

Figure 3-13. Combined treatment with MCT1 and biguanides further reduce proliferation of breast cancer cell lines. Proliferation rates of indicated breast cancer cell lines after five days of treatment with DMSO, MCT1i (IC50), metformin (IC50), metformin + MCT1i (IC50 for both), or phenformin (IC50), phenformin + MCT1i (IC50 for both). MCT1i was replenished every day. Errors bars denotes standard error of mean. * denotes $p < 0.05$, and ** denotes $p < 0.01$.

DISCUSSION

In the present study we investigated the role of MCT1 in breast cancer proliferation.

Here we show that MCT1 is critical for proliferation of glycolytic breast cancer cells. Our studies have found that MCT1 loss of function consistently reduces pyruvate export, increases oxygen consumption, and reduces proliferation rates. Dual treatment of AZD3965 with metformin or phenformin further reduces proliferation rates, presumably by blocking the compensatory switch to oxidative metabolism caused by MCT1 inhibition to sustain proliferation (Figure 3-14). Our results imply an important role for pyruvate export in promoting proliferation and reducing oxidative metabolism in glycolytic breast cancer cell lines. However, the mechanism by which blocking pyruvate export may impact proliferation remains unclear -- modulation of cellular redox status, intracellular pH, and/or ATP levels could be involved. Additionally, the mechanism by which MCT1 inhibition leads to increased cellular respiration requires further investigation. Pyruvate export inhibition may lead to increased entry of pyruvate carbons into the mitochondria to provide more substrate for oxidative phosphorylation. However, our preliminary studies tracing the fate of ^{13}C-glucose metabolites, and specifically pyruvate, in MCT1-inhibited cells have yielded varying results across the breast cancer cell lines tested. Also, elevated oxygen consumption rates are observed at 24 hours post AZD3965 treatment, but not at 30 minutes or 4 hours post treatment (Figure 2-4), suggesting that the effect on respiration is not direct but rather through programmed changes in transcription. Consistent with this notion, genes involved in oxidative phosphorylation are enriched in breast cancer cells after 24 hours AZD3965 treatment (Figure 2-3). These changes in gene expression may occur through an unknown mechanism downstream of MCT1 inhibition and reduction of pyruvate export, or may simply be a cellular adaptation to survive MCT1 inhibition. It will be interesting

to determine whether similar changes in gene expression also happen in tumors of breast cancer patients treated with AZD3965.

Doherty et al. recently found that MCT1 inhibition blocks lactate transport and decreases glycolysis to ultimately trigger cancer cell death in lymphoma and breast cancer cells (Doherty et al., 2014), however we did not observe reduced lactate export, decreased glycolysis, or increased cell death upon MCT1 inhibition in glycolytic breast cancer cell lines. One potential explanation for these discrepancies is the varying levels of MCT4 in the different cell lines used. The Burkitt lymphoma cell lines and MCF7 and T47D breast cancer cell lines used in the study by Doherty et al. expressed very little, if any, MCT4. In contrast, the relatively more glycolytic breast cancer cell lines used in our study - SUM149PT, SUM159PT, and HS578T (Figure 1-1) - expressed measurable amounts of MCT4 (Figure 3-9). MCT4 expression is likely responsible for continued lactate transport which likely sustains the glycolytic flux and survival of glycolytic breast cancer cell lines in the context of MCT1 inhibition.

Previous reports have found that MCT1 and MCT4 are commonly coexpressed in tumors (Choi et al., 2014; Kim et al., 2015). In support of this notion, we have found that MCT1 and MCT4 are often coexpressed at the mRNA level in patient breast and lung tumors (Figure 3-14). Examination of MCT1 and MCT4 mRNA levels across cancer cell lines shows a high number of cancer cell lines with dual expression of MCT1 and MCT4, and another population with high expression of MCT1 only (Figure 3-14). While several previous studies have found that MCT1 modulates cancer cell lactate transport in the absence of MCT4 expression, our results support a lactate-transport independent role for MCT1 in promoting proliferation of cancer cells with naturally-derived dual MCT1/MCT4 expression. Future experiments on patient-derived primary

breast cancers that exclusively express MCT1, MCT4, or both together, are needed to more clearly delineate the roles of MCT1 versus MCT4 in tumor metabolism and growth.

AZD3965 is thought to kill tumor cells reliant on glycolysis through inhibition of lactate transport (Doherty et al., 2014; Polanski et al., 2014). However, our data suggests that AZD3965 does not reduce lactate export, glycolytic flux, or survival of glycolytic breast cancer cell lines coexpressing MCT1 and MCT4 *in vitro*, but still impacts proliferation through an alternative mechanism, potentially via reduction of pyruvate export and/or induction of oxidative metabolism. In our mammary fat pad xenograft model, AZD3965 treatment blocked tumor growth despite causing a slight increase in tumor FDG uptake as measured by PET. These data support an alternative mode of action for AZD3965 than impaired glycolysis in blocking tumor growth and suggest that loss of tumor FDG uptake by PET is not a good biomarker of response to AZD3965 in breast cancer patients.

Pyruvate is a commonly secreted metabolite from cancer cell lines *in vitro* (Jain et al., 2012), however whether pyruvate is secreted from tumors *in vivo* remains unknown. Our finding that serum samples from Stage IV lung cancer patients have elevated pyruvate levels compared to serum from Stage I lung cancer patients is consistent with MCT1 modulation of tumor pyruvate export *in vivo* (Figure 2e). However, further studies are necessary to confirm MCT1-mediated pyruvate export from cancer cells within tumor tissues, and to determine whether and how pyruvate export impacts tumor growth. Our results expand upon a growing literature that MCT1 is necessary for optimal cancer cell proliferation and provide further support for use of MCT1 inhibitors as anti-cancer therapeutics.

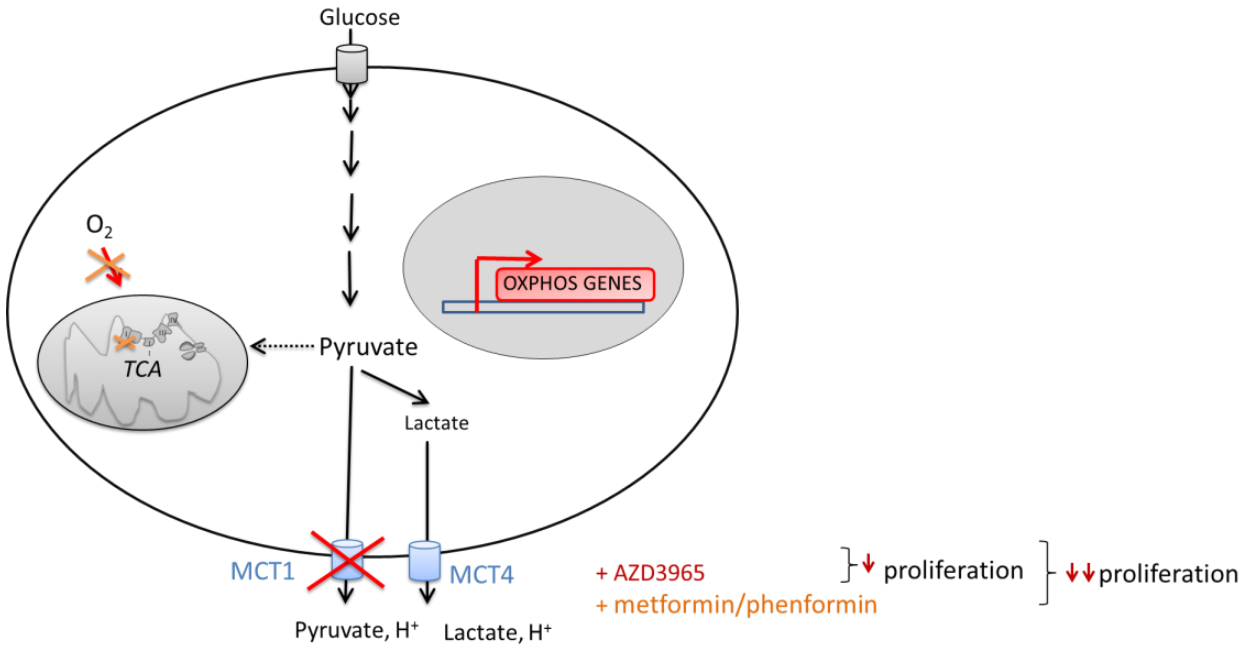

Figure 3-14. Schematic representation of the impact of MCT1 inhibition on breast cancer cell metabolism and proliferation. AZD3965 consistently reduces pyruvate export, increases oxygen consumption, and reduces proliferation rates. Dual treatment of AZD3965 with metformin or phenformin further reduces proliferation rates, presumably by blocking the compensatory switch to oxidative metabolism caused by MCT1 inhibition to sustain proliferation.

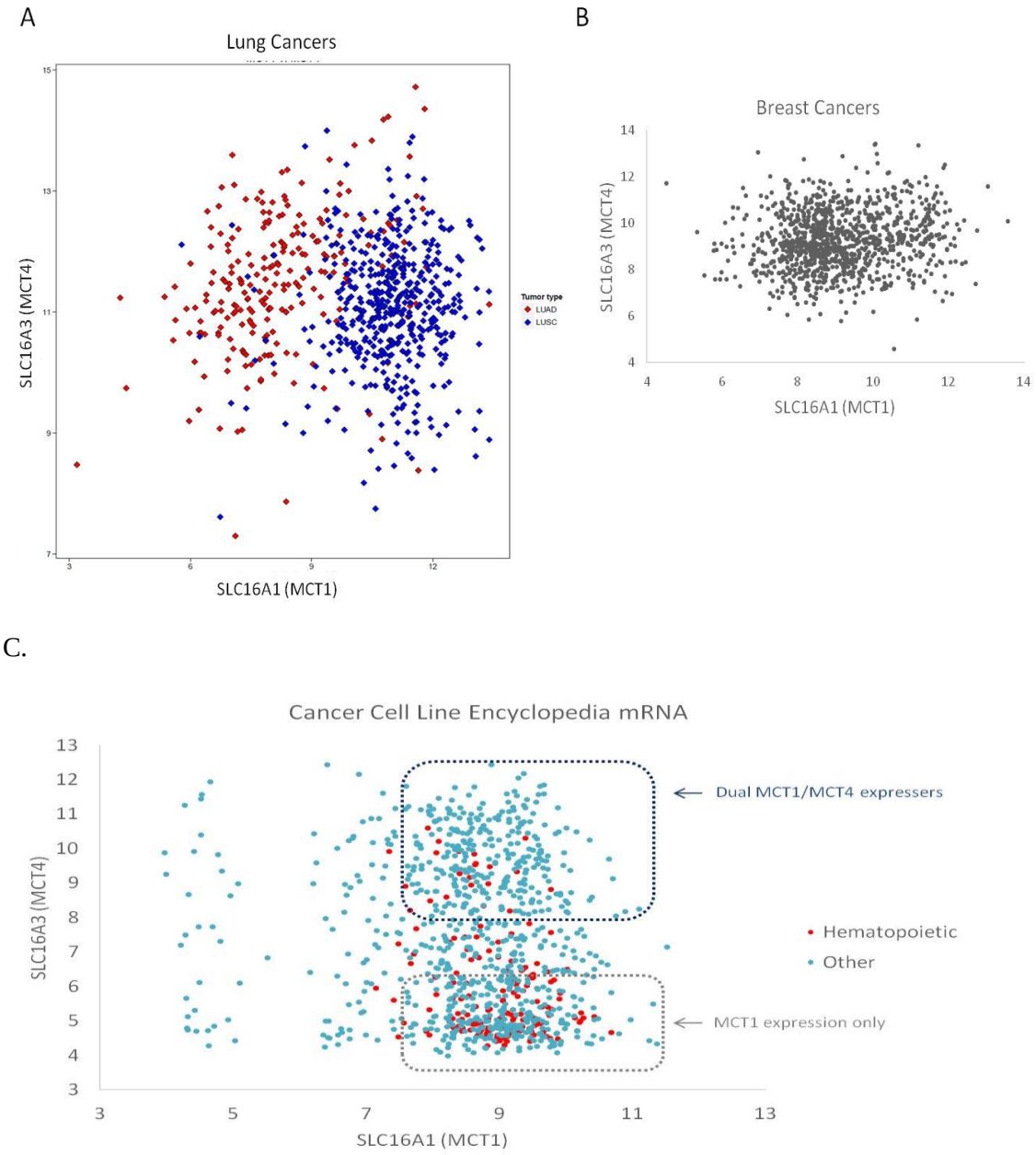

Figure 3-15. MCT1 and MCT4 mRNA is coexpressed in patient tumors and cancer cell lines. a, Scatter plot showing relative SLC16A1 mRNA (encoding MCT1) and SLC16A3 mRNA (encoding MCT4) levels from patient lung adenocarcinomas (red dots) and lung squamous cell carcinomas (blue dots). b, Scatter plot showing relative SLC16A1 and SLC16A3 mRNA levels in breast cancers. c, Scatter plot showing relative levels of SLC16A3 and SLC16A1 in cancer cell lines.

MATERIALS AND METHODS

Cell Proliferation Measurements

For cell proliferation measurements, $1x10^4$– $2x10^4$ cells were seeded in triplicate in 6-well plates and accurate cell counts were obtained using a Coulter particle analyser after a 5-day period. For the inhibitor treated cells, MCT1i was replenished daily. For the metformin and phenformin treated cells, cells were treated once at the beginning of the experiment. Dual treated cells were treated once with metformin or phenformin, while MCT1i was replenished daily. For the methyl-pyruvate and methyl-lactate treated cells, cells were treated daily.

FACS Analysis

Cell cycle analysis was performed as described previously (Krishan, 1975) and by BrdU staining (BD Pharmagin). Cell viability was assessed using an apoptosis detection kit (BD Pharmingen).

Xenograft Models

Two different breast cancer tumor xenograft models were generated. The first set of xenograft models were generated by injecting 5×10^5 of scramble stable knockdown cells in the right mammary fat pad of female NSG mice, and 5×10^5 of MCT1 stable knockdown cells in the left mammary fat pad. Mice were monitored daily for tumor development. For the second set of xenograft models 1×10^6 SUM149PT cells were inject into the right mammary fat pad of female NSG mice. Half of the mice were treated with MCT1i (AZD3965) once tumors reached a size of 5mm in diameter, and were treated twice daily by oral gauvage. Half of the mice were treated as control mice with an equal volume of vehicle. Tumor size was monitored every other day with calipers.

MicroPET/CT Imaging

For microPET imaging, animals were anesthetized with 1.5% isoflurane, USP (Phoenix Pharmaceutical Inc.) and injected intravenously with 200 uCi ^{18}F-FDG. PET imaging was conducted on a Focus 220 microPET scanner (Siemens) and, subsequently, CT recorded using a MicroCAT II CT instrument (Siemens). Data was analyzed by drawing 3-dimensional ROIs using AMIDE software (Loening and Gambhir, 2003).

References

Choi, J.W., Kim, Y., Lee, J.H., and Kim, Y.S. (2014). Prognostic significance of lactate/proton symporters MCT1, MCT4, and their chaperone CD147 expressions in urothelial carcinoma of the bladder. Urology *84*, 245 e249-215.

Evans Josie M M, Donnelly Louise A, Emslie-Smith Alistair M, Alessi Dario R, Morris Andew D. Metformin and reduced risk of cancer in diabetic patients. BMJ 2005; :bmj;bmj.38415.708634.F7v1

Galluzzi, L., Kepp, O., Vander Heiden, M. G., & Kroemer, G. (2013). Metabolic targets for cancer therapy. *Nature reviews. Drug discovery*, *12*(11), 829–46. doi:10.1038/nrd4145

Halestrap, A.P., and Wilson, M.C. (2012). The monocarboxylate transporter family--role and regulation. IUBMB Life *64*, 109-119.

Kim, Y., Choi, J.W., Lee, J.H., and Kim, Y.S. (2015). Expression of lactate/H(+) symporters MCT1 and MCT4 and their chaperone CD147 predicts tumor progression in clear cell renal cell carcinoma: immunohistochemical and The Cancer Genome Atlas data analyses. Hum Pathol *46*, 104-112.

Loening, A.M., and Gambhir, S.S. (2003). AMIDE: a free software tool for multimodality medical image analysis. Mol Imaging *2*, 131-137.

Le Floch, R., Chiche, J., Marchiq, I., Naiken, T., Ilc, K., Murray, C.M., Critchlow, S.E., Roux, D., Simon, M.P., and Pouyssegur, J. (2011). CD147 subunit of lactate/H+ symporters MCT1 and hypoxia-inducible MCT4 is critical for energetics and growth of glycolytic tumors. Proc Natl Acad Sci U S A *108*, 16663-16668.

Murray, C.M., Hutchinson, R., Bantick, J.R., Belfield, G.P., Benjamin, A.D., Brazma, D., Bundick, R.V., Cook, I.D., Craggs, R.I., Edwards, S., et al. (2005). Monocarboxylate transporter MCT1 is a target for immunosuppression. Nat Chem Biol *1*, 371-376.

Polanski, R., Hodgkinson, C.L., Fusi, A., Nonaka, D., Priest, L., Kelly, P., Trapani, F., Bishop, P.W., White, A., Critchlow, S.E., et al. (2014). Activity of the monocarboxylate transporter 1 inhibitor AZD3965 in small cell lung cancer. Clin Cancer Res *20*, 926-937.

Vander Heiden, M. G., Cantley, L. C., & Thompson, C. B. (2009). Understanding the Warburg effect: the metabolic requirements of cell proliferation. *Science (New York, N.Y.)*, *324*(5930), 1029–33. doi:10.1126/science.1160809

Warburg, O. On the origin of cancer cells. *Science* **123**, 309–314 (1956)

Xu, X., Duan, S., Yi, F., Ocampo, A., Liu, G.-H., & Izpisua Belmonte, J. C. (2013). Mitochondrial regulation in pluripotent stem cells. *Cell metabolism*, *18*(3), 325–32. doi:10.1016/j.cmet.2013.06.005

Future Directions

In addition to finding that MCT1 is highly correlative with glycolytic metabolism and tumor malignancy in breast cancer cells and patients, we found that MCT1 is critical for pyruvate export and proliferation of glycolytic breast cancer cells (schematic representation in Figure 3-14). MCT1 loss of function consistently reduces pyruvate export, increases oxygen consumption, and reduces proliferation rates. Dual treatment of AZD3965 with metformin or phenformin further reduces proliferation rates, presumably by blocking the compensatory switch to oxidative metabolism caused by MCT1 inhibition to sustain proliferation. Our findings imply an important role for pyruvate export in promoting proliferation and reducing oxidative metabolism in glycolytic breast cancer cell lines. However, the mechanism by which blocking pyruvate export may impact proliferation remains unclear. Here we will discuss potential further work that could help elucidate MCT1's role in cancer.

Investigating cellular redox status and oxidative stress upon MCT1 inhibition

The mechanism by which blocking pyruvate export impacts proliferation remains unclear. The changes in ATP and the redox ratio may provide evidence for how the metabolic pathways are being affected by MCT1 inhibition, as ATP levels and the NAD+/NADH ratio can regulate key glycolytic enzymes. Oxidative stress by increased pyruvate entry into the mitochondria for oxidative phosphorylation could also directly affect proliferation of cells. Accurate measurements of ROS, NADP+/NADPH levels and glutathione levels would be needed to determine their role on proliferation upon MCT1 inhibtion.

Investigating the mechanism by which MCT1 inhibition leads to increased cellular respiration

The mechanism by which MCT1 inhibition leads to increased cellular respiration requires further investigation. Pyruvate export inhibition may lead to increased entry of pyruvate carbons into the mitochondria to provide more substrate for oxidative phosphorylation. However, our preliminary studies tracing the fate of ^{13}C-glucose metabolites, and specifically pyruvate, in MCT1-inhibited cells have yielded varying results across the breast cancer cell lines tested. Also, elevated oxygen consumption rates are observed at 24 hours post AZD3965 treatment, but not at 30 minutes or 4 hours post treatment (Fig. 3c), suggesting that the effect on respiration is not direct but rather through programmed changes in transcription. Consistent with this notion, genes involved in oxidative phosphorylation are enriched in breast cancer cells after 24 hours AZD3965 treatment (Figure 3b and Supplemental Figure 7). These changes in gene expression may occur through an unknown mechanism downstream of MCT1 inhibition and reduction of pyruvate export, or may simply be a cellular adaptation to survive MCT1 inhibition. It will be interesting to determine whether similar changes in gene expression also happen in tumors of breast cancer patients treated with AZD3965.

Separating the role of MCT1 and MCT4

Previous reports have found that MCT1 and MCT4 are commonly coexpressed in tumors (Choi et al., 2014; Kim et al., 2015). In support of this notion, we have found that MCT1 and MCT4 are often coexpressed at the mRNA level in patient breast and lung tumors (Supplementary Fig. 15). Examination of MCT1 and MCT4 mRNA levels across cancer cell lines shows a high number of cancer cell lines with dual expression of MCT1 and MCT4, and another population with high expression of MCT1 only (Supplementary Fig. 15). While several previous studies have found that MCT1 modulates cancer cell lactate transport in the absence of MCT4 expression, our results support a lactate-transport independent role for MCT1 in

promoting proliferation of cancer cells with naturally-derived dual MCT1/MCT4 expression. Future experiments on patient-derived primary breast cancers that exclusively express MCT1, MCT4, or both together, are needed to more clearly delineate the roles of MCT1 versus MCT4 in tumor metabolism and growth.

Effect of MCT1 inhibition on pyruvate in breast cancer tumors in *vivo*.

Pyruvate is a commonly secreted metabolite from cancer cell lines *in vitro* (Jain et al., 2012), however whether pyruvate is secreted from tumors *in vivo* remains unknown. Our finding that serum samples from Stage IV lung cancer patients have elevated pyruvate levels compared to serum from Stage I lung cancer patients is consistent with MCT1 modulation of tumor pyruvate export *in vivo* (Figure 2e). However, further studies are necessary to confirm MCT1-mediated pyruvate export from cancer cells within tumor tissues, and to determine whether and how pyruvate export impacts tumor growth. Our results expand upon a growing literature that MCT1 is necessary for optimal cancer cell proliferation and provide further support for use of MCT1 inhibitors as anti-cancer therapeutics.

References

Choi, J.W., Kim, Y., Lee, J.H., and Kim, Y.S. (2014). Prognostic significance of lactate/proton symporters MCT1, MCT4, and their chaperone CD147 expressions in urothelial carcinoma of the bladder. Urology *84*, 245 e249-215.

Kim, Y., Choi, J.W., Lee, J.H., and Kim, Y.S. (2015). Expression of lactate/H(+) symporters MCT1 and MCT4 and their chaperone CD147 predicts tumor progression in clear cell renal cell carcinoma: immunohistochemical and The Cancer Genome Atlas data analyses. Hum Pathol *46*, 104-112.

Jain, M., Nilsson, R., Sharma, S., Madhusudhan, N., Kitami, T., Souza, A.L., Kafri, R., Kirschner, M.W., Clish, C.B., and Mootha, V.K. (2012). Metabolite profiling identifies a key role for glycine in rapid cancer cell proliferation. Science *336*, 1040-1044.